PLOS ONE

RESEARCH ARTICLE

Site-specific gene expression profiling as a novel strategy for unravelling keloid disease pathobiology

N. Jumper[1], T. Hodgkinson[1,2], R. Paus[3], A. Bayat[1,3]*

1 Plastic and Reconstructive Surgery Research, University of Manchester, Oxford Rd, Manchester, United Kingdom, **2** Centre for Tissue Injury and Repair, University of Manchester, and MAHSC, Manchester, United Kingdom, **3** Centre for Dermatology Research, University of Manchester, and MAHSC, Manchester, United Kingdom

* Ardeshir.Bayat@manchester.ac.uk

Citation: Jumper N, Hodgkinson T, Paus R, Bayat A (2017) Site-specific gene expression profiling as a novel strategy for unravelling keloid disease pathobiology. PLoS ONE 12(3): e0172955. doi:10.1371/journal.pone.0172955

Editor: Michael A. Tangrea, Sinai Hospital, UNITED STATES

Received: August 1, 2016

Accepted: February 13, 2017

Published: March 3, 2017

Data Availability Statement: All microarray files are available from the ArrayExpress database (accession number(s) E-MTAB-4945 (identifier)).

Funding: Industry funded (GlaxoSmithKline). The funders had no role in study design, data collection and analysis, decision to publish, or preparation of the manuscript.

Competing interests: GlaxoSmithKline partially funded this research but there are no financial competing interests, non-financial, personal or professional competing interests and does not alter

Abstract

Keloid disease (KD) is a fibroproliferative cutaneous tumour characterised by heterogeneity, excess collagen deposition and aggressive local invasion. Lack of a validated animal model and resistance to a multitude of current therapies has resulted in unsatisfactory clinical outcomes of KD management. In order to address KD from a new perspective, we applied for the first time a site-specific *in situ* microdissection and gene expression profiling approach, through combined laser capture microdissection and transcriptomic array. The aim here was to analyse the utility of this approach compared with established methods of investigation, including whole tissue biopsy and monolayer cell culture techniques. This study was designed to approach KD from a hypothesis-free and compartment-specific angle, using state-of-the-art microdissection and gene expression profiling technology. We sought to characterise expression differences between specific keloid lesional sites and elucidate potential contributions of significantly dysregulated genes to mechanisms underlying keloid pathobiology, thus informing future explorative research into KD. Here, we highlight the advantages of our *in situ* microdissection strategy in generating expression data with improved sensitivity and accuracy over traditional methods. This methodological approach supports an active role for the epidermis in the pathogenesis of KD through identification of genes and upstream regulators implicated in epithelial-mesenchymal transition, inflammation and immune modulation. We describe dermal expression patterns crucial to collagen deposition that are associated with TGFβ-mediated signalling, which have not previously been examined in KD. Additionally, this study supports the previously proposed presence of a cancer-like stem cell population in KD and explores the possible contribution of gene dysregulation to the resistance of KD to conventional therapy. Through this innovative *in situ* microdissection gene profiling approach, we provide better-defined gene signatures of distinct KD regions, thereby addressing KD heterogeneity, facilitating differential diagnosis with other cutaneous fibroses via transcriptional fingerprinting, and highlighting key areas for future KD research.

our adherence to all PLOS ONE policies on sharing data and materials.

Abbreviations: DEG, differentially expressed genes; ECM, extracellular matrix; EMI, epithelial-mesenchymal interactions; EMT, epithelial-mesenchymal transition; IL, interleukin; KD, keloid; Kd, keloid dermis; KE, keloid epidermis; LCM, laser capture microdissection; MET, mesenchymal-epithelial transition; NS, normal skin; disease; TGF, transforming growth factor; UV, ultraviolet; 2D, 2-dimensional.

Introduction

Keloid disease (KD) is a fibroproliferative cutaneous tumour of ill-defined pathogenesis characterised by clinical, behavioural and histological heterogeneity [1]. Keloid scars, consisting mostly of hyalinised collagen bundles, spread beyond the boundaries of the original wound resulting in "claw-like" or "cheloide" invasions into adjacent normal skin. KD research has been hindered by lack of a validated animal model, a paucity of tissue for experimentation secondary to ethical concerns over high rates of recurrence following excision [2] and both inter-patient and inter-lesional heterogeneity [3]. The multitude of available therapies, including first-line non-invasive treatments (compression garments, physiotherapy, camouflage), second-line treatments such as corticosteroid injection or cryotherapy and more extreme experimental agents including chemotherapy and radiotherapy, indicate the lack a gold standard effective treatment option for KD [4]. In an effort to overcome this, our previous studies including others have considered KD in terms of different lesional sites within the keloid scar: intralesional (centre), perilesional (margin) and extralesional (adjacent normal skin) [5].

The evidence for site-specific KD is threefold. Macroscopically, the centre is often pale soft and shrunken when compared with the raised erythematous margin. Microscopically, there are differences with respect to epidermal thickness, inflammatory infiltrate, collagen ratios and cellularity [6, 7]. Finally, on a molecular level, these sites have been shown to differ with regard to cell cycle phase and apoptotic factor expression [8]. While this site-specific approach has highlighted the diversity within KD, the use of whole tissue biopsy and monolayer culture fail to accurately reflect the *in situ* expression of this unique 3D microenvironment.

Therefore, in addition to site-specific, the second aspect of our approach was to examine *in situ* signalling. We achieved this by combining laser capture microdissection (LCM) and transcriptomic array profiling (**Fig 1A**). To date, LCM has played a limited role in cutaneous wound healing but given its success both in other areas of fibrosis research as well as benign and malignant dermatological conditions [9–11], we felt it was an ideal methodological platform for application to KD. This approach also allowed us to focus on individual expression in different regions of the keloid scar without the need for "averaging out" of signals commonly consequential to whole tissue biopsy analysis or the altered expression that can result from the *in vitro* environment of monolayer cell culture [12].

The overall aim of this study was not to validate specific theories but to apply an innovative hypothesis-free and compartment-specific approach to KD. Thus, the first aim was to compare this combined LCM and microarray (*in situ*) approach to both whole tissue biopsy and monolayer culture methods of analysing gene expression (**Fig 1B**). The second aim was to enrich the data in terms of gene ontology, in an effort to explore the biological processes within different lesional sites of the keloid scar. Finally, we aimed to examine differentially expressed genes (DEG) from each site of both epidermis and dermis compared with micro-dissected normal skin (NS), to identify pathways for potential diagnostic and therapeutic exploitation.

We show that our *in situ* approach most accurately reflects the *in vivo* environment without missing functionally important DEG through dilution and averaging out. These DEG indicate an activated epidermis with a potential for epithelial-mesenchymal transition (EMT) and expose dermal collagen-promoting molecules of which *TGF*β is an integral component but which remain overlooked in KD. The sensitivity of this technique allowed us to unveil another piece of the complex inflammatory network contributing to KD, unravel some of the elements contributing to therapeutic resistance and strengthen the argument for a stem cell population in KD [13].

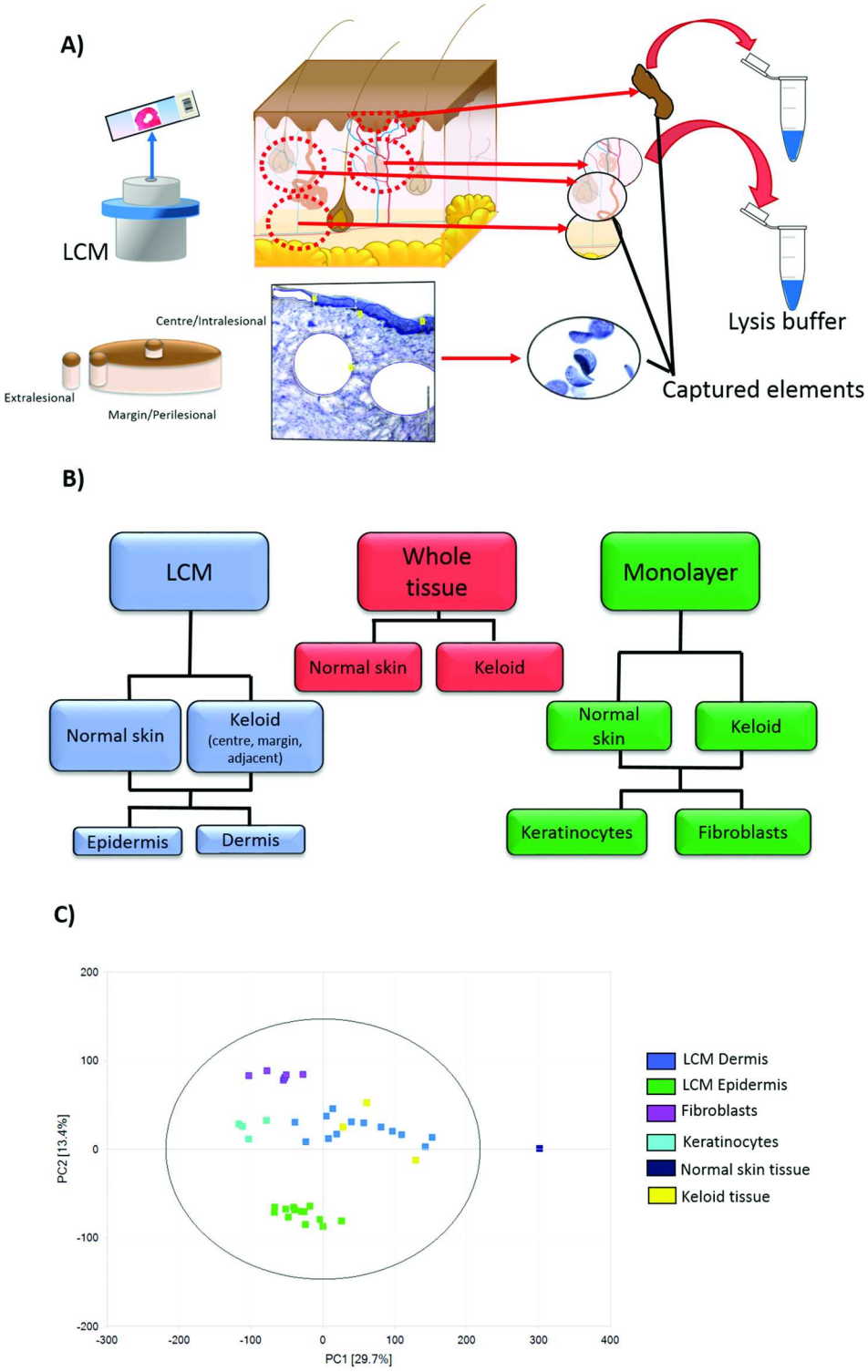

Fig 1. Experimental approaches for the comparison of site-specific keloid disease with normal skin. A) Schematic diagram demonstrating laser capture microdissection (LCM) of epidermis and dermis for each of the shown keloid biopsy sites, centre (intralesional), margin (perilesional) and keloid-adjacent normal skin (extralesional). LCM was performed for keloid sites and normal skin. As shown, the elements pertaining to portions of each compartment (epidermis separate to dermis) were delineated, cut using ultraviolet (UV) laser and catapulted into the cap of an overhanging tube, where images confirmed their presence. This was then immersed in lysis buffer and stored at -80˚C. B) The three methods of experimental technique used to

compare keloid with normal skin: LCM, whole tissue biopsy and 2D monolayer cell culture. C) Principal component analysis (PCA) plot for the gene expression derived from experimental approaches described above. The epidermal and dermal samples are evident as separate clusters as are the laser captured material and the monolayer culture samples.

doi:10.1371/journal.pone.0172955.g001

Materials and methods

Study approval

Keloid and NS tissue were harvested at the time of surgery following full verbal and written consent obtained in accordance with the Declaration of Helsinki. The North West Research Ethics Committee (NorthWest of England, UK) approved this specific study (ethical Reference number. 11/NW/0683). In total there were 8 of each NS and keloid tissue donors used for microarray, with additional samples included for supporting data (**S1 Table**). The scar was considered to be keloid if it fulfilled the following criteria: growth beyond the boundaries of the original wound, failure to regress with time, present for at least one year and lesions that would recur with excision alone [14, 15].

Tissue processing

Tissue biopsies were taken from keloid scar centre, margin and extralesional sites (**Fig 1A**). NS biopsies were from patients undergoing routine non-oncologic elective surgery. Biopsies were immediately preserved in either RNA stabilisation solution (RNA*later*®, Life technologies Ltd, Paisley, UK) or 10% (v/v) neutral buffered formalin (Sigma-Aldrich, UK). The RNA stabilised samples were OCT (optimum cutting temperature)-embedded (CellPath, UK) and snap frozen before being stored at -80˚C.

Laser capture microdissection

Serial 8μm cryosections (Leica CM3050S, UK) of OCT-embedded keloid and NS samples were cut onto specialised polyethylene naphthalate (PEN) membrane slides (Carl Zeiss, UK). To differentiate epidermis from dermis, whilst preserving tissue RNA integrity, a rapid staining protocol was performed (LCM Staining Kit, Ambion, Austin TX, USA) according to the manufacturer's instructions [16, 17]. Using a P.A.L.M. LCM microscope (Carl Zeiss MicroBeam 4.2, Germany) epidermis and dermis of each sample was laser cut and catapulted away from the slide into separate overhanging microtube caps (AdhesiveCap 200 Opaque, Carl Zeiss Microscopy Ltd, Cambridge, UK). Multiple 'elements' were captured from each tissue section of least three sequential sections from each patient, ensuring adequate biological representation. The captured tissue was mixed with lysis buffer (Buffer RLT with 1% 2-mercaptoethanol, RNeasy Micro Kit, Qiagen, UK) and stored at -80˚C until extraction according to manufacturer's instructions (RNeasy Micro Kit, Qiagen, UK). Following extraction, the samples were again stored at -80˚C [18].

RNA amplification and microarray

Extracted RNA was amplified using the Ovation® Pico WTA system v2 kit (NuGen Technologies, USA) and purified with QIAquick PCR purification kit (Qiagen, UK), according to manufacturer's instructions. Prior to microarray, RNA quantity was estimated using a microvolume spectrophotometer (ThermoScientific NanoDrop 2000 UV-vis, USA). Agilent SureTag DNA labelling and hybridisation kit were used according to manufacturer's instructions and slides (SurePrint G3 Human GE 8x60K V2, Agilent Technologies, USA) scanned using an Agilent Microarray Scanner G2505c [19–21].

Quantitative Real-Time Polymerase Chain Reaction (qRT-PCR)

qRT-PCR was performed using the Lightcycler® 480 II platform (Roche Diagnostics, UK) as previously described [22]. A final reaction volume of 10μl contained normalised cDNA, LightCycler®480 probes master mix, forward and reverse primers, nuclease-free water (Qiagen, UK) and the associated probe from the Universal Probe Library (Roche, UK). Reactions were performed in triplicate with two house-keeping genes (RPL32 and GAPDH) for relative quantification. Amplified targets were analysed using the Lightcycler® II software (1.5.0 SP3, Roche, UK).

Cell culture

Primary keratinocytes and fibroblasts were established as previously described [22, 23]. In brief, tissue was cut and incubated in Dispase II (10mg/ml; Roche Diagnostics, UK) at 37˚C. The epidermis was stripped, diced and incubated in TrypLE™Express (ThermoFisher Scientific, USA) with serum-free keratinocyte medium (Epilife®, Invitrogen Life Technologies, ThermoFisher Scientific, USA) for one hour before neutralising, centrifugation and dispersion into T25 flasks. The dermis was further incubated in collagenase before adding to complete DMEM and grown in flasks. Medium was changed every 48hrs until confluent. Passages 1–3 were used. Cells were lysed and RNA extracted using Qiagen RNeasy Micro Kit, according to manufacturer's instructions.

Statistical analysis

Data was extracted from the raw files and initial microarray analysis performed using Array studio v7.2 (OmicSoft Corporation, USA) and the data quantile normalised. A linear model was then fitted to the $\log_2$ transformed data for which both p-value and False Discovery Rate (FDR), controlled for using Benjamini-Hochberg method, were calculated for each group comparison [24]. Least squared means (LS means) and 95% confidence interval (where n>1) were outputted for each group. The data was then filtered using the following criteria: maximum median signal intensity >8 (leaving 46802 probe sets), p-value <0.05, fold change >2 and for individual genes of interest, q-value < 0.05 (**S3 and S4 Figs**). Lists of DEG were loaded into Ingenuity Pathway Analysis (IPA, Qiagen). IPA was chosen as the primary mode of enrichment analysis as all pathways, ontologies and interactions are manually curated and have supporting literature data behind them, thus providing a very robust and standardised platform for interpreting differential gene lists from transcriptomic studies. A full table of expanded gene names for each symbol discussed below can be found in **S2 Table**.

For qRT-PCR, expression was normalised against internal controls and $\Delta\Delta C_T$ calculated. Statistical analysis was performed using Student's *t*-test and one way ANOVA with Tukey post-hoc correction (SPSS, IBM), where p-value <0.05 was considered significant [25]. Data are represented as mean ± SEM.

Results & discussion

Microarray analysis reveals variable differential gene expression based on experimental approach

Initial analysis was conducted to define site-specific gene expression, determine relationships between experimental approaches and establish networks based on correlation clustering. We compared gene expression for both epidermis and dermis between different sites within the keloid lesion, based on their expression difference over their NS epidermal and dermal

Table 1. Number of significant differentially expressed genes within each comparative microarray group (filtered for fold change > 2 and p-value < 0.05).

Harvest method	Comparison	Total sig. changes	Up	Down	FDR-corrected (q < 0.5)
LCM	*Keloid centre vs normal epidermis*	1165	591	574	18
LCM	*Keloid margin vs normal epidermis*	911	562	349	11
LCM	*Keloid extralesional vs normal epidermis*	1425	608	817	28
LCM	*Keloid centre vs normal dermis*	3640	1795	1845	1085
LCM	*Keloid margin vs normal dermis*	3818	1852	1966	882
LCM	*Keloid extralesional vs normal dermis*	3313	1549	1765	423
Monolayer	*Keloid vs normal keratinocytes**	356	207	149	21
Monolayer	*Keloid vs normal fibroblasts*	247	146	101	3
Whole tissue	*Keloid vs normal skin**	12527	7583	4944	9076

FDR, false discovery rate; LCM, laser capture microdissection.

*keloid keratinocyte and whole tissue normal skin biopsy $n = 1$.

doi:10.1371/journal.pone.0172955.t001

counterpart. Additionally, we analysed whole tissue biopsy and monolayer culture (keratinocyte and fibroblast) expression for both KD and NS. The number of significant DEG within these comparative groups as well as their direction of change is shown in Table 1.

Principal component analysis (PCA) was used to assess technical variability in the microarray QC metrics; the expected 5% of samples (2/40) lay outside the 95% confidence interval but were from two separate donors and therefore not excluded. Following quantile normalisation [26], probe sets were filtered by calculating maximum group median and removed if minimum signal intensity was < 8 (on $\log_2$ scale), leaving 24,228 probes (approximately 40%). PCA was employed to ascertain relationships between sample groups and compare variability between replicate arrays and experimental conditions [27].

This plot indicated the most significant variability existed between different cell types, that is epidermis and dermis or keratinocyte and fibroblast, which fell into separate clusters (X-axis) but variability was also found between the *in situ* micro-dissected cell layer and it's *in vitro* monolayer culture equivalent i.e. epidermis and keratinocyte (Y-axis) (Fig 1C). Some of this variability could be attributed to the differentiation state of keratinocytes. Additionally, while keratinocytes and fibroblasts constitute the major cell type in the epidermis and dermis respectively, the *in situ* tissue layer will comprise additional cells that contribute to expression. Therefore, as expected, the epidermal layer and dermal layer, as well as their constituent cells, differed in their expression profiles. Interestingly however, this analysis also indicated there was differential gene expression dependent on the experimental approach, such that keratinocyte expression (derived from monolayer cell culture) differed from that of the laser-captured *in situ* epidermal expression. The same was true for the culture-derived fibroblasts and micro-dissected dermis.

Using weight gene correlation network analysis (WGCNA), a soft threshold was established and the microarray data was clustered into an eigengene networks, thereby allowing gene ontology enrichment based on consensus modules. This identified three key modules where KD expression diverged most significantly from that of NS. Transforming growth factor beta (*TGF*β), *Wnt*, Phosphoinositide 3-kinase (*PI3K/AKT*) and Focal adhesion kinase (*FAK*) signalling were preserved across the three modules as were remodelling and cell adhesion processes (S1 Fig). This analysis overview resonated with the current literature on mechanisms underlying keloid pathobiology, thus validating our data.

An *in situ* microdissection approach leads to improved accuracy and sensitivity of differential gene expression over monolayer culture and whole tissue biopsy dissection

We compared differential gene expression of KD with NS samples from whole tissue biopsy, monolayer culture and *in situ* LCM, in order to determine both experimental approach most representative of the keloid microenvironment and also the method most likely to identify important or novel biomarkers/pathways.

This was achieved by first comparing the DEG produced by each approach to establish any overlap or disparity. As seen from Venn diagrams [28] (**Fig 2A and 2B**) only 0.2% and 0.5% of DEG were common to all three approaches in epidermis and dermis respectively. Given that whole tissue biopsy incorporates both epidermis and dermis, it's clear the microdissection approach produces the highest number of DEG specific to either layer. This data was uploaded to Ingenuity Pathway Analysis (IPA) Software (Ingenuity® Systems, www.ingenuity.com), which organised the DEG into known canonical pathways, biological functions, upstream regulators and interactive networks. For both epidermis and dermis, while all three groups captured the predominant epidermal (*PI3K*, *MAPK/ERK*) and dermal (*TGF*β) expression, the microdissection approach incorporated the essential elements of both whole tissue and monolayer expression, providing a more complete picture of overall expression. Also, there were a significant number of DEG in the microdissection group alone that were not identified with monolayer or were averaged out in whole tissue analysis. This is due to the dilution effect of looking at whole tissue as transcriptomes from different cell types that are pooled together, which reduces the sensitivity.

In addition to comparing DEG between approaches, we examined the difference in degree of expression. For this, we compared expression between *in situ* micro-dissected dermis, captured by LCM and 2D *in vitro* cultured fibroblasts for genes known to be dysregulated in KD. Representative graphs are shown in **Fig 3A,** which demonstrate significantly increased expression of both *TGFβ1* and *CTGF* with *in vitro* monolayer fibroblasts compared with micro-dissected tissue, for both KD and NS. This was also true for the rest of the genes analysed (**S2 Fig**). This might be somewhat expected considering 2D culture is a static physical environment, maintained with exogenous often undefined (foetal bovine serum) medium that lacks stimuli from other cell types and can alter cell morphology/polarity and phenotype [29]. These factors affect expression, with monolayer often resulting in higher-magnitude changes [12]. In this case, the overexpression seen with monolayer culture vs *in situ* microdissection approach falsely minimises the degree of gene upregulation in keloid compared with NS dermis. Given the sensitivity and accuracy of degree of expression, we concluded our *in situ* LCM approach would be the most fruitful going forward.

In situ microdissection reveals keloid sites contribute disproportionately to differential gene expression

Given the advantages of LCM *in situ* tissue capture, we then sought to use this technique to define the contribution of different sites within the keloid lesion to specific gene expression as well as distinguish epidermal from dermal signalling. To achieve this, we performed qRT-PCR for a number of genes known to be dysregulated in KD (**S2 Fig**), of which two are represented in **Fig 3B.** We demonstrated that *TGFβ1* signalling is largely attributed the keloid centre as compared to the margin or extralesional dermis and identified IL-8 upregulation as localised largely to keloid centre epidermis. By examining the keloid as separate components we were able to attribute specific expression to key sites, with the precision necessary for therapeutic targeting.

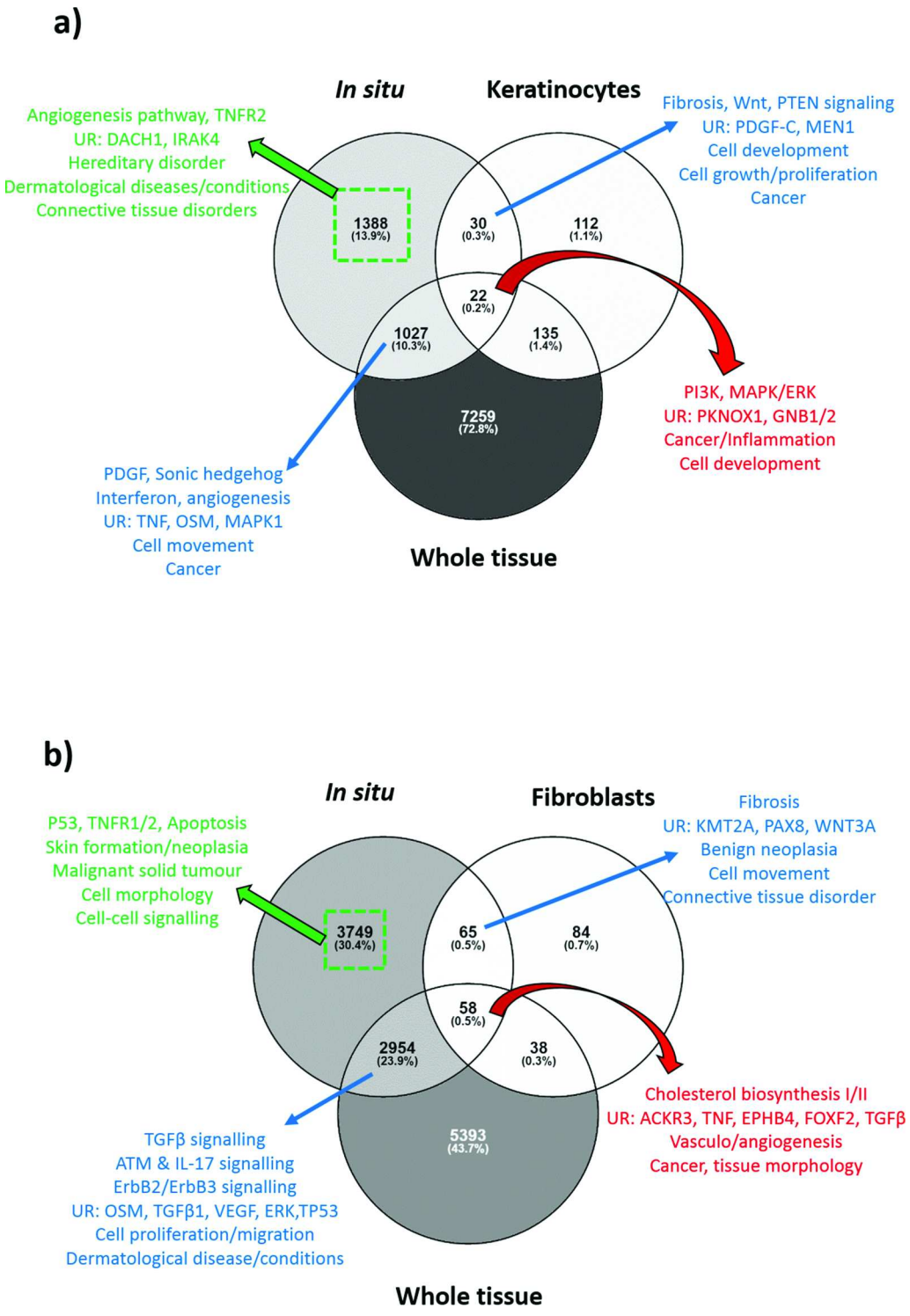

Fig 2. Comparison of *in situ* microdissection KD expression to whole tissue biopsy and monolayer culture expression. (A) Venn diagram comparing microdissected keloid epidermal expression to whole tissue and keratinocyte culture expression. The red arrow and text indicates where all 3 methods overlap and the results of enrichment using Ingenuity Pathway Analysis (IPA) for this group. The blue arrows and text indicate where either alternative method overlaps with *in situ* expression and the associated enrichment for that group. The green arrow and text indicates the enrichment analysis result for the 1388 genes that were identified in the microdissection group alone. (B) Venn diagram comparing micro-dissected keloid dermal expression to whole

tissue and fibroblast culture expression. The red arrow and text indicates where all 3 methods overlap and the results of enrichment using IPA for this group. The blue arrows and text indicate where either alternative method overlaps with *in situ* expression and the associated enrichment for that group. The green arrow and text indicates the enrichment analysis result for the 3749 genes that were identified in the microdissection group alone. ACKR3, atypical chemokine receptor 3; ATM, ataxia telangiectasia mutated; DACH1, dachshund family transcription factor 1; EGF, epidermal growth factor; EPHB4, ephrin (EPH) receptor B4; FOXF2, forkhead box F2; GNB, guanine nucleotide binding protein (G protein); IL, interleukin; IRAK4, interleukin-1 receptor associated kinase-4; KMT2A, lysine (K)-specific methyltransferase 2A; MAPK/ERK, mitogen-activated protein kinase; MEN1, menin; OSM, oncostatin M; PAX8, paired box 8; PDGF, platelet-derived growth factor; PI3K, phosphoinositide 3-kinase; PKNOX1, PBX/knotted 1 homeobox 1; PTEN, phosphatase and tensin homolog; TGFβ, transforming growth factor beta; TNF, tumour necrosis factor; TNFR2, tumour necrosis factor receptor 2; TP53, tumour protein 53; UR, upstream regulators; VEGF, vascular endothelial growth factor.

doi:10.1371/journal.pone.0172955.g002

Enrichment of the site-specific microdissected keloid epidermis suggests an active role in the pathogenesis of keloid disease

We employed LCM to look at the epidermis as a separate entity from the dermis, which highlighted a number of DEG that have previously been overlooked with alternative methods of dissection. Generally for the epidermis, the margin and centre shared more upregulated genes than either did with the extralesional tissue, however, the centre and extralesional sites had more downregulated genes in common than either did with the margin. To interpret the expression differences and similarities between epidermal sites, the data was uploaded to IPA (**Fig 4A**). The centre keloid epidermis (KE) alone was characterised by fibrosis, inflammation and apoptosis. When taken together with the margin KE, collagen turnover and inflammation were distinguished as key events. The upstream regulators *TGF*β, PRRX1 and *DAB2* supported an EMT hypothesis. The identification of angiogenesis and cell-cell signalling networks as well as *VEGF* as an upstream regulator upheld the margin as the active site of keloid and emphasised the role of the epidermis in this process [7]. There were 232 DEG common to all three sites of the KE compared with NS epidermis (NSE). Interestingly, retinoate biosynthesis was revealed to be the top canonical pathway in this group with key molecules including *IFN*, *TNF*, *HOXA13* and *MAPK*1 proposed as upstream regulators.

Enrichment of the site-specific micro-dissected keloid dermis supports the presence of epithelial-mesenchymal transition, immune modulation and keloid margin-related migration

With regard to the keloid dermis (Kd), there was a significant increase in shared expression between centre and margin than with extralesional tissue, for both up and downregulated genes (**Fig 4B**). Compared with NS dermis (NSD), there were 1208 DEG common to centre and margin Kd, where *TGF*β signalling was identified by IPA as a top canonical pathway, as might be expected in KD. The proposed upstream regulators in this group included *SNAI1*, SNAI2, *SMO*, *Wnt3A* and *BMP2*, which not only influence cell growth, proliferation and fibrosis but are also all involved in EMT [30–33]. When we examined all three sites of the microdissected Kd together, we identified angiogenic factors (*HIF1α*, *ANGPT2*) and migration regulators (ErbB, SERPINE1) to be in common. Enrichment of the margin Kd highlighted migration regulators (ErbB & tight junction signalling), the potential existence of embryonic stem cell markers (*OCT4*), which were previously identified in the microvessels of keloid associated lymphoid tissue [34] and immune response modulators (*IL-17*, *IL-12* & *IRF7* [35]), much of which were shared at its overlap with extralesional dermis expression. These processes are consistent with the signature expected of an invading tumour margin [36].

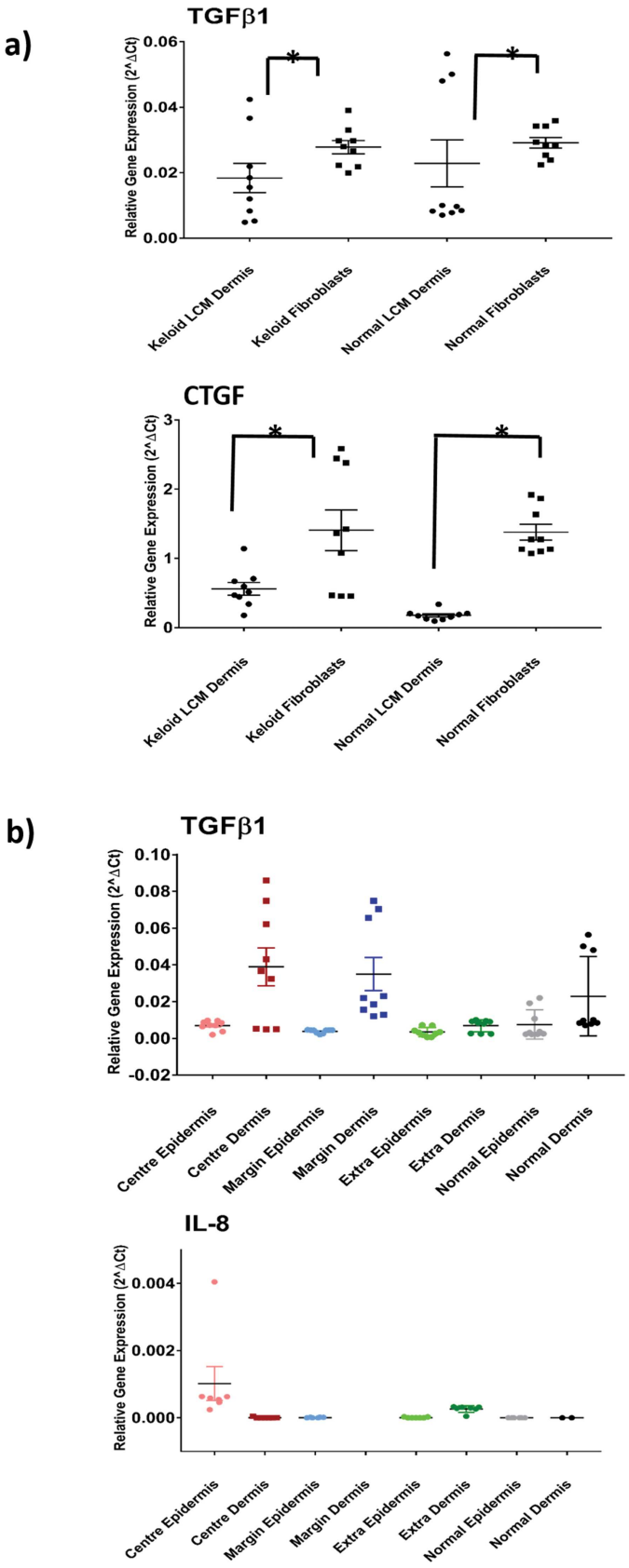
a)
TGFβ1
Relative Gene Expression (2^ΔCt)
0.06
0.04
0.02
0.00
*
*
Keloid LCM Dermis
Keloid Fibroblasts
Normal LCM Dermis
Normal Fibroblasts
CTGF
Relative Gene Expression (2^ΔCt)
3
2
1
0
*
*
Keloid LCM Dermis
Keloid Fibroblasts
Normal LCM Dermis
Normal Fibroblasts
b)
TGFβ1
Relative Gene Expression (2^ΔCt)
0.10
0.08
0.06
0.04
0.02
0.00
-0.02
Centre Epidermis
Centre Dermis
Margin Epidermis
Margin Dermis
Extra Epidermis
Extra Dermis
Normal Epidermis
Normal Dermis
IL-8
Relative Gene Expression (2^ΔCt)
0.004
0.002
0.000
Centre Epidermis
Centre Dermis
Margin Epidermis
Margin Dermis
Extra Epidermis
Extra Dermis
Normal Epidermis
Normal Dermis

Fig 3. Site-specific contribution to differential gene expression in KD. (A) Comparison of gene expression between laser-captured dermal tissue (*in situ*) and fibroblasts for both keloid and normal skin. qRT-PCR graph for both *TGFβ1* and *CTGF* (additional examples found in **S2A Fig**). All data are mean ± SEM for at least three independent experiments. B) qRT-PCR for *TGFβ1* and interleukin-8 (*IL-8*) showing relative contributions of different keloid sites to overall expression and comparison with normal skin (additional genes available in **S2B Fig**). Data are mean ± SEM where * p-value <0.05 using Student's *t* test and ANOVA with Tukey post hoc correction. CTGF, connective tissue growth factor; TGFβ, transforming growth factor beta.

doi:10.1371/journal.pone.0172955.g003

The microdissected keloid epidermis expresses an activated, pro-inflammatory profile with the potential for epithelial-mesenchymal transition

In addition to expression overview and enrichment, we investigated the individual DEG of micro-dissected sites for both KE and Kd compared with NS. A full list of the top 100 upregulated and 50 downregulated genes is available for each site in **S5–S16 Figs**. Additionally, a detailed table of expanded genes for each of the symbols below can be found in **S2 Table.**

For the epidermis, the most significantly dysregulated genes were common to all three sites and indicated an activated, hyper-proliferative, pro-inflammatory and mesenchymally-poised epithelium. Keratin 6α and 6β were both significantly upregulated in all three epidermal sites, supporting the hyper-proliferation seen on keloid histology [1]. *K6* is induced in keratinocytes following injury where it is associated with migration through *Src* regulation [37, 38]. This activated epidermal expression [39] is reversible on wound closure and NSE (except the hair follicle) does not express *K6* [40]. Mucin-like 1 (*MUCL1*) was also significantly overexpressed in the micro-dissected epidermis and has been associated with aggressive breast tumorigenesis and recurrence [41]. Interestingly, it was demonstrated that *MUCL1* may be required for proliferation of *ErbB2*-overexpressing breast cells [41], which was identified as overexpressed here in margin Kd. The inflammation-associated scavenger receptor *CD36* is also a marker of epidermal activation and not present in NS keratinocytes without specific stimuli [42]. It has been shown to disappear from hypertrophic scars with age whereas keloid scars maintained their *CD36* expression [43, 44], which is supported here by *CD36* upregulation in all 3 sites of the KE. The role of *CD36* in signal transduction suggests it may contribute to epithelial-mesenchymal signalling and it has been shown to affect the secretion of *TGFβ1* [45], which is dysregulated in KD [46, 47].

The presence of EMT in KD, is supported by our finding of *S100A8*, *WDR66* and *AKR1B10* overexpression in all 3 micro-dissected epidermal sites. The knockdown of keratinocyte *S100A8*, recently shown to be upregulated in both keloid and hypertrophic scar epidermis, resulted in a failure to activate co-cultured fibroblasts and reduction in dermal fibrosis [48]. As a mediator of neutrophil migration [49, 50], *S100A8* is found in the supra-basal epidermis following injury, but gradually returns to baseline in a normally healed wound [51]. The role of *S100A8* in conversion of wounded keratinocytes to a migratory phenotype may represent a potential link to EMT and contribution to tumorigenesis [51]. Also implicated in EMT is the protein WDR66, which in oesophageal carcinoma has been shown to affect vimentin and occludin expression where its knockdown attenuated both cell proliferation and motility [52]. While we did not find altered vimentin expression, we did identify upregulation of fibronectin (*FN1*) ($p = 0.06$) and α-*SMA/ACTA2* ($p = 0.033$) in the micro-dissected centre KE. Our data also identified a significant upregulation of *AKR1B10* (as well as *AKR1B1* and *AKR1B15*) in all three sites of the KE. This enzyme has a key role in the metabolism of retinoic acid (RA) and our recent study found the induced overexpression of *AKR1B10* in NS keratinocytes resulted in significant downregulation of E-cadherin [23]. Additionally, the treatment of keloid fibroblasts with AKR1B10-overexpressing keratinocyte medium resulted in upregulation of *TGFβ1*,

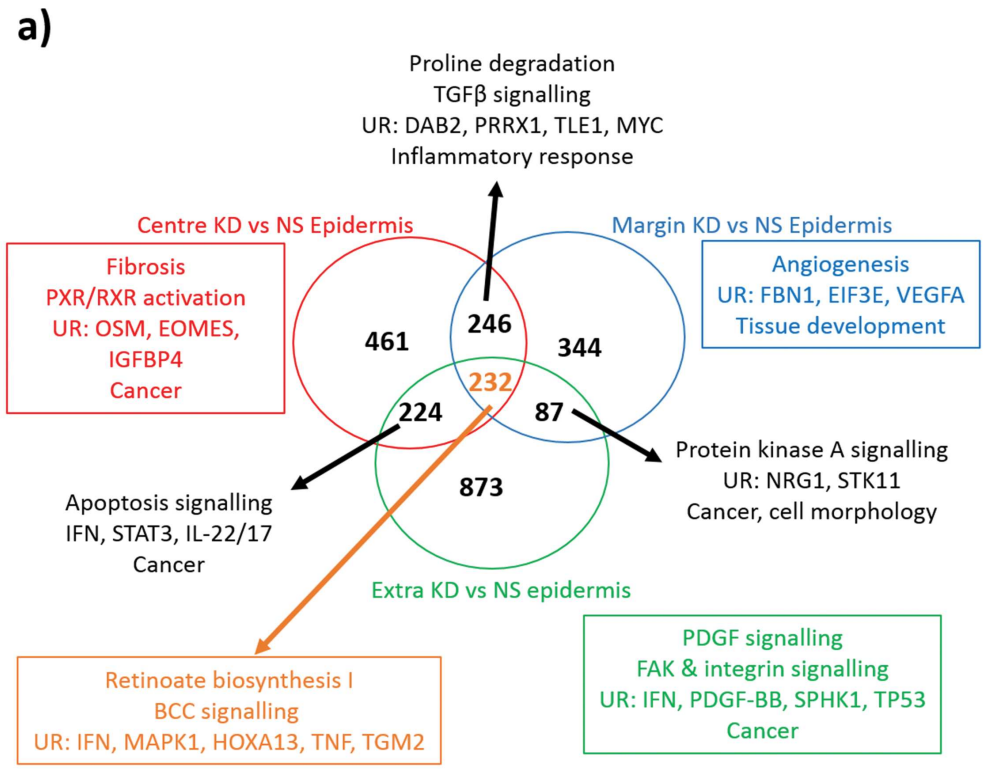
a)
Proline degradation
TGFβ signalling
UR: DAB2, PRRX1, TLE1, MYC
Inflammatory response
Centre KD vs NS Epidermis
Margin KD vs NS Epidermis
Fibrosis
PXR/RXR activation
UR: OSM, EOMES, IGFBP4
Cancer
Angiogenesis
UR: FBN1, EIF3E, VEGFA
Tissue development
461
246
344
232
224
87
873
Protein kinase A signalling
UR: NRG1, STK11
Cancer, cell morphology
Apoptosis signalling
IFN, STAT3, IL-22/17
Cancer
Extra KD vs NS epidermis
Retinoate biosynthesis I
BCC signalling
UR: IFN, MAPK1, HOXA13, TNF, TGM2
PDGF signalling
FAK & integrin signalling
UR: IFN, PDGF-BB, SPHK1, TP53
Cancer

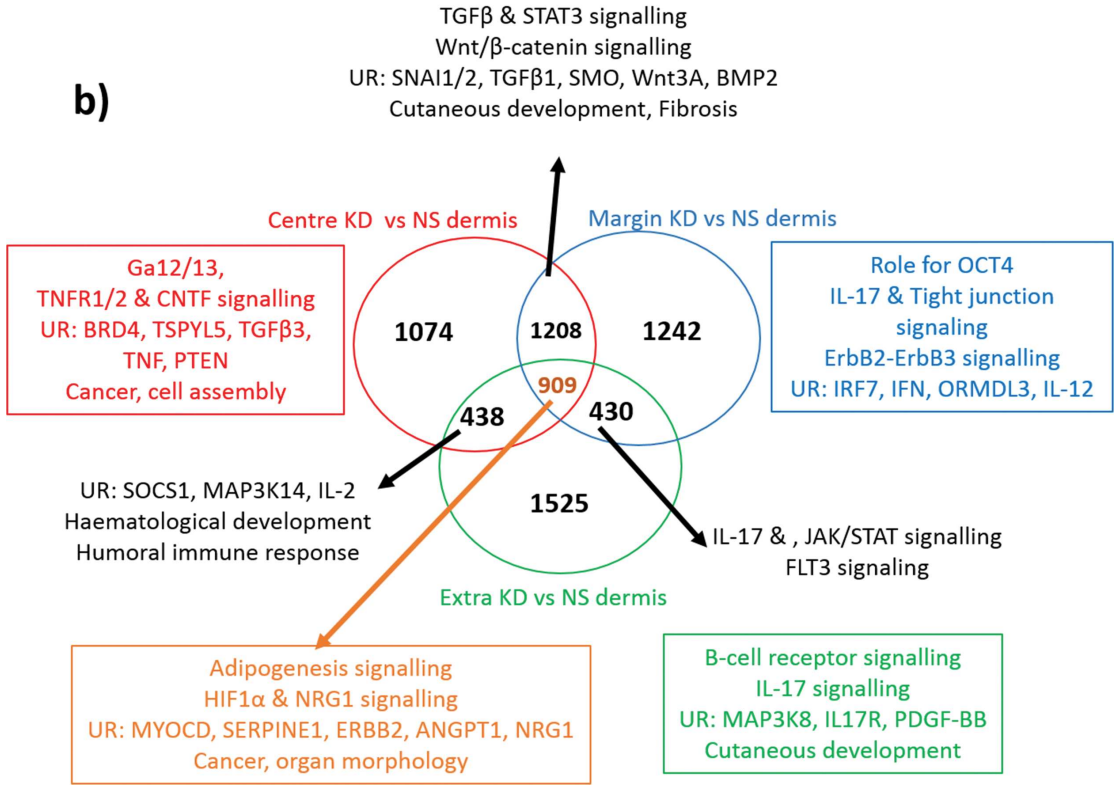
b)
TGFβ & STAT3 signalling
Wnt/β-catenin signalling
UR: SNAI1/2, TGFβ1, SMO, Wnt3A, BMP2
Cutaneous development, Fibrosis
Centre KD vs NS dermis
Margin KD vs NS dermis
Ga12/13,
TNFR1/2 & CNTF signalling
UR: BRD4, TSPYL5, TGFβ3, TNF, PTEN
Cancer, cell assembly
Role for OCT4
IL-17 & Tight junction signaling
ErbB2-ErbB3 signalling
UR: IRF7, IFN, ORMDL3, IL-12
1074
1208
1242
909
438
430
1525
UR: SOCS1, MAP3K14, IL-2
Haematological development
Humoral immune response
IL-17 & , JAK/STAT signalling
FLT3 signaling
Extra KD vs NS dermis
Adipogenesis signalling
HIF1α & NRG1 signalling
UR: MYOCD, SERPINE1, ERBB2, ANGPT1, NRG1
Cancer, organ morphology
B-cell receptor signalling
IL-17 signalling
UR: MAP3K8, IL17R, PDGF-BB
Cutaneous development

Fig 4. Gene enrichment analysis of microdissected site-specific keloid disease. Venn diagram of keloid disease (KD) centre, margin and extralesional expression vs normal skin (NS), where A) refers to the epidermis and B) refers to the dermis. The red circle and text refer to the centre vs NS alone, the blue to margin vs NS and the green to extralesional keloid site alone vs NS. The black arrows and text refer to the enrichment results of where the expression of the indicated sites overlap. The orange arrow and text refers to the enrichment analysis of the indicated number of genes in common to all three keloid sites over NS. In both A) and B) enrichment analysis was performed with Ingenuity Pathway Analysis (IPA) and included canonical pathways, diseases & functions, networks and upstream regulators of interest. ANGPT2, angiopoietin 2; BCO1, beta-carotene oxygenase 1; BMP2, bone morphogenetic protein 2; BRD4, bromodomain containing 4; DAB2, Dab, mitogen-responsive phosphoprotein, homolog 2 (drosophila); EGF, epidermal growth factor; EIF3E, eukaryotic translation initiation factor 3 subunit E; EOMES, eomesodermin; FBN1, fibrillin 1; FLT3, fms related tyrosine kinase 3; GSTP1, glutathione s-transferase pi 1; HIF, hypoxia-inducible factor; HOXA13, homeobox A13; IFN, interferon; IGFBP, insulin-like growth factor binding protein; IL, interleukin; IRF, interferon regulatory factor; JAK, janus kinase; MAPK, mitogen-activated protein kinase; MYC, c-Myc; MYOCD, myocardin; NRG1, neuregulin-1; OCT4, octamer-binding transcription factor 4; ORMDL3, orosomucoid like 3; OSM, oncostatin M; PDGF, platelet-derived growth factor; PTEN, phosphatase and tensin homolog; PXR, pregnane X receptor; PRRX1, paired related homeobox 1RXR, retinoid X receptor; SERPINE1(PAI-1), serpin peptidase inhibitor. Clade E (plasminogen activator inhibitor 1); SMO, smoothened; SNAI1, snail family zinc finger 1; SOCS, suppressor of cytokine signalling; SPHK, sphingosine kinase; STAT, signal transducer and activator of transcription; STK11, serine/threonine kinase 11; TGF, transforming growth factor; TGM2, transglutaminase 2; TLE1, transducin like enhancer of split 1; TNF(R), tumour necrosis factor (receptor); TP53, tumour protein 53; TSPYL5, testis-specific protein Y encoded like 5; UR, upstream regulators; VEGF, vascular endothelial growth factor.

doi:10.1371/journal.pone.0172955.g004

Collagen I and collagen III, supporting a role for pathological epithelial-mesenchymal interactions (EMI) in keloid pathogenesis.

EMI encompass the essential cross-talk that governs the epidermal-dermal relationship in the skin and in addition to a multitude of essential organ development and physiologic processes, are essential for successful wound healing. Dysregulation of the processes involved in EMI (e.g. malfunction of negative feedback loops) can lead to abnormal wound healing and fibrosis or contribute to tumorigenesis [53, 54]. Previous exploration into the contribution of these EMI to KD, have highlighted the significance of the epidermis in the formation and maintenance of this fibrotic scar [55, 56].

BMP2, a member of the *TGF*β superfamily, was downregulated in our microarray data and has been shown to attenuate renal fibrosis, by reversing *TGF*β1-induced EMT and cellular fibrotic markers [32]. Similarly, the loss of claudin-4 (*CLDN4*) and *CLDN23*, integral components of the tight junctions that maintain epithelial cell contacts [57] and downregulated here in the micro-dissected KE, are strongly implicated in EMT, potentially through E-cadherin modulation and thought to be negatively regulated by *TGF*β [58–60]. We also identified significant upregulation of *NOTCH4* in all 3 epidermal sites and centre and margin Kd, which is linked with cancer stem cell activity and interestingly has very recently been associated with mesenchymal-epithelial transition (MET) [61, 62].

A role for EMT has previously been implicated in the pathogenesis of KD [63, 64]. EMT is a potentially reversible process whereby epithelial cells lose adhesion properties (downregulation E-cadherin, *CLDN4* and *CLDN23*) and gain migratory and invasive characteristics, transforming into mesenchymal cells (upregulation *FN1* and *ACTA2*) [65]. Here, we present DEG that in combination support a role for EMT or at least "partial EMT" in KD (**Fig 5A**).

Microdissected keloid dermis expression reinforces the significance of TGFβ in KD pathogenesis through its regulation of the collagen network

Collagen is the major structural protein of the ECM and fibrillar collagens (type I & III) are present in abundance in KD [1]. Fibroblasts are the most common producers of collagen and are subject to complex autocrine and paracrine cytokine signals to regulate its formation, of which TGFβ is crucial [66, 67]. In combination with these cytokines there are a number of enzymes and proteins that through cleavage or binding can affect collagen turnover [68].

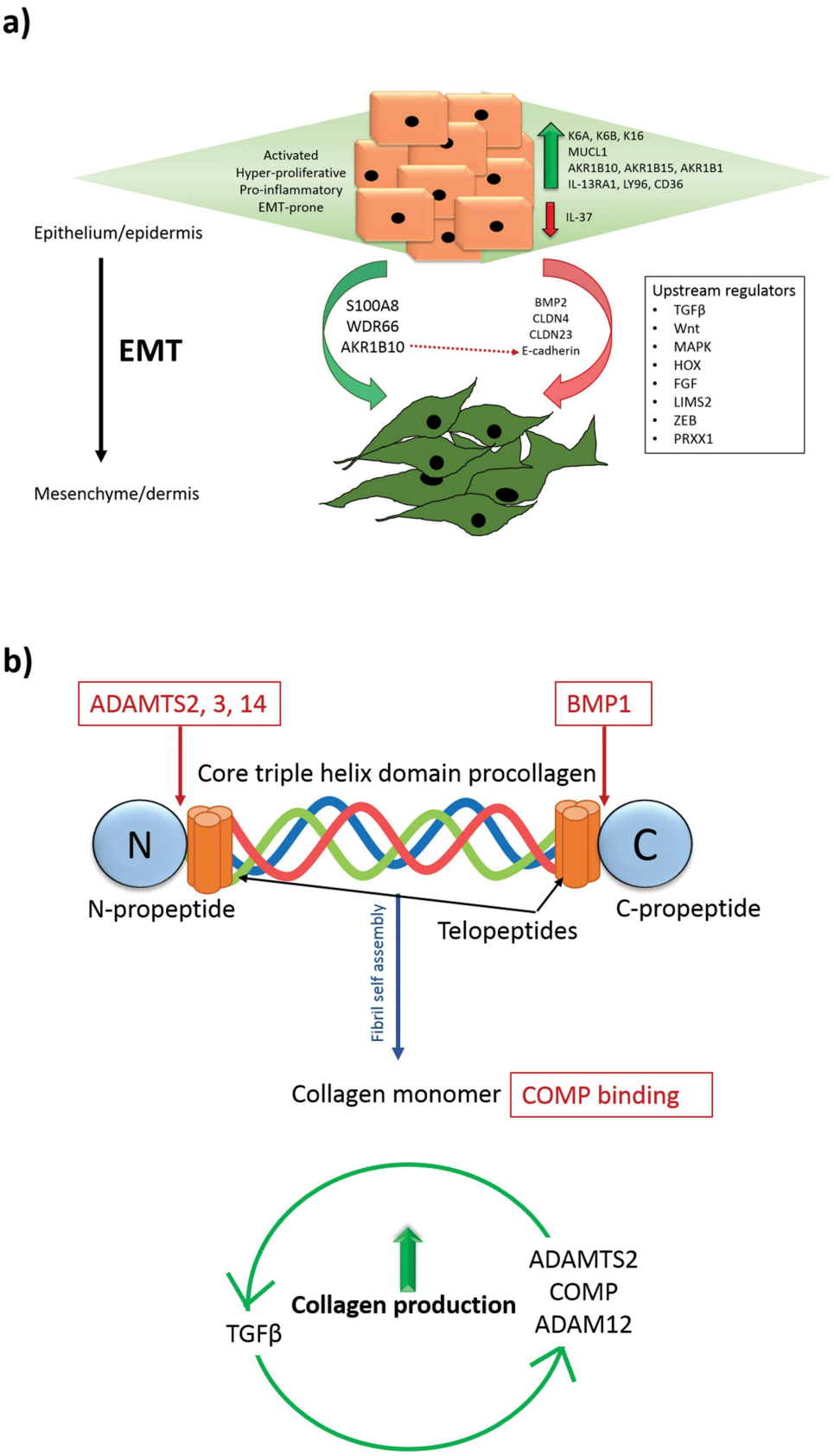
a)
Activated
Hyper-proliferative
Pro-inflammatory
EMT-prone
K6A, K6B, K16
MUCL1
AKR1B10, AKR1B15, AKR1B1
IL-13RA1, LY96, CD36
IL-37
Epithelium/epidermis
EMT
Mesenchyme/dermis
S100A8
WDR66
AKR1B10
BMP2
CLDN4
CLDN23
E-cadherin
Upstream regulators
TGFβ
Wnt
MAPK
HOX
FGF
LIMS2
ZEB
PRXX1
b)
ADAMTS2, 3, 14
BMP1
Core triple helix domain procollagen
N
C
N-propeptide
C-propeptide
Telopeptides
Fibril self assembly
Collagen monomer
COMP binding
Collagen production
TGFβ
ADAMTS2
COMP
ADAM12

Fig 5. *In situ* microdissection expression contributing to epithelial-mesenchymal transition (EMT) and collagen production in KD. A) Schematic diagram of the differentially expressed genes (DEG) in KD that contribute to an activated, hyper-proliferative and inflammatory epidermis. Also depicted are DEG from our microarray data hypothesised to contribute to EMT through upregulation (green arrow) or downregulation (red arrow), which are described along with the upstream regulators identified on enrichment analysis of our microarray data and which have been previously implicated in the EMT process. B) Schematic diagram depicting where ADAMTS and BMP cleave the procollagen peptides to form tropo-collagen and allow collagen fibril assembly necessary for collagen turnover. Once a collagen monomer, it may bind COMP. Collagen production in KD may be increased by the potential existence of positive feedback loops between ADAMTS2/COMP/ADAM12 and TGFβ. ADAM, a disintegrin and metalloproteinase; ADAMTS, a disintegrin and metalloproteinase with thrombospondin motifs; AKR1B10, aldo-keto reductase family 1, member 10; BMP, bone morphogenetic protein; CLDN, claudin; COMP, cartilage oligomeric protein; FGF, fibroblast growth factor; HOX, homeotic gene subset; IL, interleukin; K, keratin; LIMS2, LIM zinc finger domain containing 2; MAPK, mitogen-activated protein kinase; MUCL1, mucin-like 1; S100A8, S100 calcium-binding protein A8; TGFβ, transforming growth factor beta; WDR66, WD repeat domain 66; ZEB, zinc finger E-box-binding proteins.

doi:10.1371/journal.pone.0172955.g005

Within the microdissected centre and margin Kd, we identified dysregulation of a number of members of the ADAMTS family of enzymes, which are associated with tissue morphogenesis, remodelling, inflammation and angiogenesis [69]. Of these, *ADAMTS14* and *ADAMTS2* were the most significantly upregulated and are both pro-collagen N peptidases (pNP), responsible for the cleavage of type I and II pro-collagen necessary for fibril assembly and collagen biosynthesis (**Fig 5B**) [70, 71]. Interestingly, *BMP1*, responsible for the cleavage of the C-proteinase is also upregulated in centre and margin Kd (**Fig 5B**) [72]. The *ADAMTS* enzymes are associated with Dupuytren's disease [73], craniofacial fibrosis [74], Ehlers Danlos [75] and cancer [76, 77], with *ADAMTS2*-knockout mice demonstrating skin fragility [78] and reduced liver fibrosis *in vivo [79]*. More recently, studies have argued for *ADAMTS* involvement in a positive *TGF*β feedback loop, whereby *ADAMTS2* is induced by but also targets *TGF*β [80, 81]. To date the best-described inhibitor of *ADAMTS* is *TIMP3* [70, 82, 83], which we found to be significantly downregulated in our microarray data in both centre ($p = 0.026$) and margin ($p = 0.037$) Kd. Interestingly, we identified upregulation of disintegrin and metalloproteinase *ADAM12*, the member of a family closely related to the ADAMTS group of proteins and which was also suggested to be involved in a positive feedback loop with *TGF*β, resulting in continuous collagen production [84]. This proteinase is upregulated in several cancers and fibroses and was previously identified as upregulated in the keloid centre, where it was thought contribute to tissue remodelling [5, 85, 86]. Through its association with *TGF*β, *ADAM12* has been implicated in EMT [87].

Also involved in collagen fibril assembly, is cartilage oligomeric matrix protein (*COMP*), which was significantly upregulated in both centre and margin Kd. *COMP* binds with affinity to collagens, especially collagen I, and has been previously identified in KD [88], where similar to *ADAMTS* it may be involved in a positive *TGF*β feedback loop [89, 90]. Another member of the collagen matrix regulators and also previously investigated in KD is collagen triple helix repeat containing 1 (*CTHRC1*), which was demonstrated to decrease *TGF*β-induced keloid fibroblast collagen I expression [91]. However, despite the seemingly contradictory descriptions of the negative effect of *CTHRC* on collagen I expression [92, 93], it has been widely correlated with tissue invasion and migration, where its expression was induced by *TGF*β [94, 95]. Here, we found *CTHRC1* significantly upregulated in microdissected centre and margin Kd. This may represent the result of a feedback mechanism to counteract the expression of *TGF*β, *ADAMTS* and *COMP* but without further investigation the mechanism underlying *CTHRC1* overexpression in keloid scars remains to be fully elucidated. In addition to *ADAMTS*, *ADAM12*, *COMP* and *CTHRC1*, we identified asporin (*ASPN*) and Wnt1-inducible-signaling pathway protein 1 (*WISP1*) as upregulated in both centre and margin Kd, which are also

correlated with *TGF*β expression. *ASPN*, a small leucine-rich proteoglycan though to regulate tumour microenvironment, is known to bind *TGF*β [96, 97] and has previously been found to be upregulated in the margin of KD [98]. The pro-proliferative *WISP1*, a member of the matricellular CCN family, was detected in Dupuytren's disease [99] and is strongly associated with liver [100] and lung fibrosis, where it was induced by *TGF*β1 [101] and implicated in EMT.

*TGF*β is considered a master regulator in KD, involved in several positive and negative feedback loops that culminate in the net production of excess ECM through angiogenesis, proliferation, inflammation, differentiation processes and as indicated here, collagen deposition (**Fig 5B**) [102, 103]. *TGF*β is also a major player in EMT, where it effects change at transcriptional and translational levels through both Smad and non-Smad pathway signalling [104–108]. While *TGF*β*3* was significantly upregulated in the keloid centre and margin on microarray, *TGF*β1 was confirmed as upregulated in Kd compared with normal skin dermis using qRT-PCR (**Fig 3A**).

In situ microdissection expression indicates the potential contribution of IL-13, IL-17 and IL-37 to the inflammatory process underlying keloid disease

The inflammatory phase of wound healing is a spatially and temporally precise process, essential to the supply of growth factor, chemokine and cytokine signalling necessary for repair. However, prolonged inflammation can result in impaired wound healing, leading to chronic wounds or excess scarring [109, 110]. KD is associated with an exaggerated inflammatory response [6, 111]. Prolongation of the inflammatory phase with extended residency of these factors promotes proliferation, angiogenesis and increased deposition of ECM [112]. Interleukins are a group of secreted cytokines central to the inflammatory process that have an incompletely understood role in KD and may represent potential therapeutic targets.

IL-13, a potent fibrosis-promoting cytokine secreted by activated T_H2 T-cells [113, 114], has been shown to increase collagen I & III production in keloid fibroblasts *in vitro* [115]. We found significant upregulation of *IL13RA1* in KE, epidermal and dermal upregulation of IL-4R and downregulation of *IL13RA2* in the microdissected Kd (**Table 2**). Together, *IL-13RA1* and *IL-4R* bind both *IL-13* and *IL-4* with high affinity to activate *JAK/STAT6* signalling (**Fig 6**) [116]. *IL-13RA2* is largely considered a high affinity decoy receptor thought to inhibit *IL-13* signalling *in vivo* and protect against fibrosis [117, 118]. Although this has been disputed [116], *IL-13* inhibition attenuated fibrosis and *IL-13RA2*-knockout mice have demonstrated enhanced *IL-13*-mediated responses *in vivo* [119–121]. Our current microarray findings, combined with previous evidence of KD containing an inflammatory niche populated by M2 macrophages [6], known to be *IL-13* recruited, supports an overexpression of *IL-13* in KD.

In addition to *IL-13* dysregulation, in all 3 KE sites compared with NS epidermis we identified loss of *IL-37*, a relatively new member of the interleukin-1 (*IL-1*) family, which described as anti-inflammatory has been shown to decrease the expression of *IL-6*, *IL-1*β, *TNF*α and *IL-17* [122], all of which are associated with KD [13, 112]. It is thought *IL-37* is involved in a negative feedback loop to control excess inflammation, whereby *IL-37* induction by *TNF*α or toll-like receptors (TLR) results in suppression of *TNF*α and inhibition of pro-inflammatory cytokine release (**Fig 6**) [123]. While *IL-37* itself has not previously been investigated in KD, this finding is supported by altered expression of *IL-17*, *IL-1*β and *TNF*α in our microarray data.

IL-17 signalling was dysregulated in common to both margin and extralesional Kd sites on enrichment analysis (**Fig 4B**). The pro-inflammatory *IL-17* is produced by a subset of activated CD4+ T-cells, namely T_H17 and a subset of innate lymphoid cells termed ILC3s, whose differentiation and cytokine production is regulated by a complex interplay of molecules [124–126].

Table 2. Dysregulation of cytokines in site-specific KD microarray relating to IL-13, IL-37 and IL-17. All have p-value < 0.05. See Fig 6 for relationships.

Molecule	Keloid site	Centre: direction & fold change	Margin: direction & fold change	Extralesional: direction & fold change
IL-13RA1	*Epidermis*	↑ 8.45	↑ 4.8	↑ 3
IL-13RA2	*Dermis*	↓ 10.8	↓ 8.67	↓ 9.66
IL-37	*Epidermis*	↓ 6.51	↓ 4.85	↓ 10.66
IL-17RA	*Epidermis*	-	-	↓ 2.6
IL-17RA	*Dermis*	↓ 2.9	↓ 2.35	↑ 3.36
IL-1β	*Dermis*	-	↑ 3.83	↑ 4.61
IL-23A	*Dermis*	-	-	↑ 2.73
IL-6R	*Epidermis*	-	↑ 4.06	-
IL-21R	*Dermis*	-	↑ 2.64	↑ 2.01
IL-2RA	*Dermis*	-	↑ 2.95	-
IL-4R	*Epidermis*	↑ 2.31	-	-
IL-4R	*Dermis*	↑ 5.97	↑ 11.41	↓ 4.65
IL-27	*Dermis*	↑ 2.34	↑ 1.84	↑ 2.15
STAT3	*Dermis*	-	↓ 2.02	↓ 2.1
SOCS3	*Epidermis*	-	-	↑ 3.64
SOCS3	*Dermis*	↑ 4.32	↑ 5.68	↑ 5.69
IL-8	*Dermis*	-	-	↑ 12.27
RORc	*Dermis*	↓ 4.92	-	-

IL, interleukin; R, receptor; RA, receptor alpha; A, alpha; STAT, signal transducer and activator of transcription; SOCS, suppressor of cytokine signalling; ROR, retinoid-related orphan receptor.

doi:10.1371/journal.pone.0172955.t002

Studies have shown that *IL-6* and *TGF*β initiate T_H17 differentiation, *IL-23* in an autoregulatory feedback loop with *IL-1*β is responsible for the maintenance of *IL-17* and that *IL-2*, *IL-27*, *IL-4* and *IFN*ϒ are negative regulators [124, 127]. While we know KD shows an increased T-cell infiltrate in the dermis and that there is an inflammatory niche driven by the *IL-17/IL-6* axis, the complex interplay of this signalling mechanism remains incompletely understood [6, 13, 128]. Here, we identify an imbalance in inflammatory cytokine signalling, which alters between the three KE and Kd sites compares to NS (**Table 2**). Within the literature the association between these cytokines and their regulators/substrates is described with some variability and **Fig 6** depicts an interpretation of these relationships and how they may interact in KD. The *IL-17* environment is both cell-type and context-type dependent in contribution to neutrophil recruitment, angiogenesis and invasion [129, 130]. IL-17 is known to be involved in other fibrotic conditions [131–133] and in KD it may be that *IL-17* expression differs between different sites within the keloid scar and that ongoing paracrine signalling produces the dynamic expression seen here.

The dysregulation of *IL13*, *IL-37* and *IL-17* in KD from our microarray data are likely interconnected (**Table 2**) and the mechanisms underlying modulation of KD by these interleukins requires further elucidation to determine their contribution to its pathogenesis and potential for therapeutic exploitation (**Fig 6**).

In situ microdissection analysis identifies loss of tumour suppression genes that combined with an expression profile promoting therapeutic resistance may account for currently ineffective keloid management

The failure to switch on essential genes responsible for the attenuation of processes central to fibrosis can lead to exponential growth. The loss of expression of these genes can be as

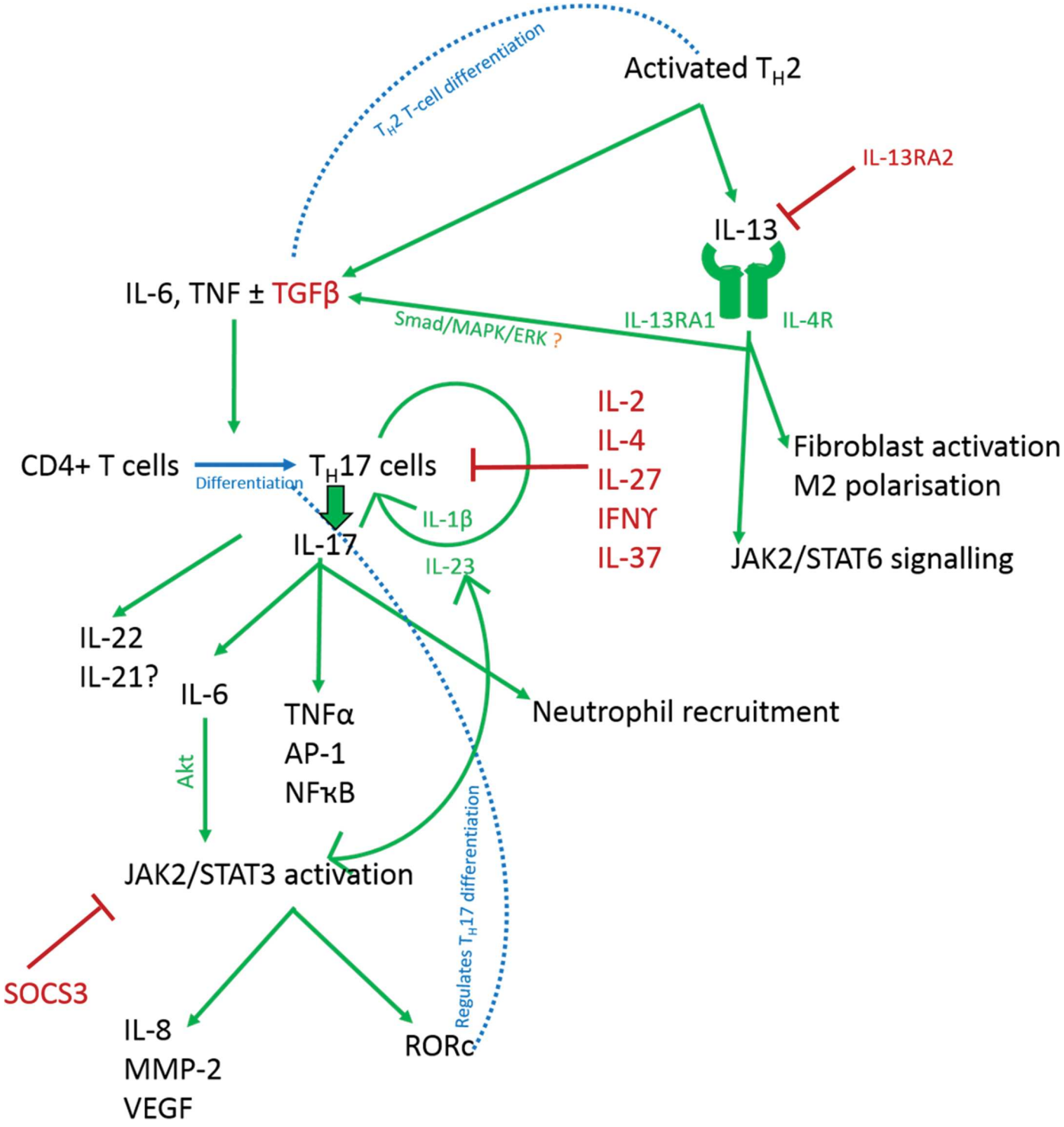

Fig 6. Cytokine relationship with potential inflammatory effects in KD. Schematic diagram of the possible relationships existing between a number of cytokines and growth factors identified as dysregulated in KD microdissected epidermis and dermis in our microarray data. This figure should be correlated with Table 2 where the direction and fold change for each of these molecules can be found for each site within keloid epidermis and dermis. AP-1, activating protein 1; IL, interleukin; INF, interferon; JAK, janus kinase; MMP, matrix metalloproteinase; NFκB, nuclear factor kappa B; ROR, retinoic acid-related orphan receptor c; STAT, signal transducer and activator of transcription; TGFβ, transforming growth factor beta; TNF, tumour necrosis factor.

doi:10.1371/journal.pone.0172955.g006

significant in the pathogenesis of KD as the overexpression of others. In this study, we identified a number of DEG previously associated with tumour suppression and drug resistance but not fully explored in KD.

Looking at the dermis, both *CEACAM1* and *SOX9* were found to be downregulated in keloid centre and margin compared with NSD. *CEACAM1*, a glycoprotein that mediates cell adhesion and immunity, is dysregulated in a number of cancers and considered a tumour suppressor gene [134–136]. Loss of *CEACAM1* has been implicated in the switch from superficial to pro-angiogenic, invasive tumour [137]. The concomitant downregulation of *SOX9* is likely to be linked given the correlation to *CEACAM1* in the literature to date [138–140].

We identified downregulation of *ATF3* in both centre and margin KE compared with microdissected NSE. Although not previously investigated in KD, this CREB family protein is downregulated in a number of cancers [141] and considered an adaptive-response gene with tumour-suppressing effects that to date, demonstrate dual-role cell-type dependency [142, 143]. *ATF3* promotion of apoptosis, a key process in prevention of growth and invasion, may result from *KLF6* induction of *ATF3* [144] or through its activation of *p53* [145]. We found a significant downregulation of *KLF6* in the centre KE ($p = 0.02$) and interestingly, *ATF3* has been shown to mediate apoptosis by anti-cancer therapies [146–148]. Also in the microdissected KE, *UGT3A2*, a member of the UDP-glycosyltransferase superfamily that plays a role in drug metabolism and which may affect detoxification of therapeutic drugs, was found to be strongly under-expressed [149, 150].

Our recent publication on the upregulation of *AKR1B10* in KE, where we hypothesised its ability to catalyse the reduction of carbonyls and xenobiotics may render keloid susceptible to chemotherapeutic resistance and thus explain some of the difficulties associated with management of KD to date [23, 151]. Both *ALDH1A1* and the aforementioned upregulation of *NOTCH4* in KE are also associated with drug resistance [152, 153]. The upregulation of these molecules and multi-drug resistant nature of keloid scars may indicate the presence of a cancer stem cell-like population within the scar, which has been touched on but not fully explored in the literature [154, 155]. Tubulin β3, class III (*TUBB3*), a cytoskeletal microtubule protein previously identified in solid tumours and extraocular fibrosis [156, 157], was also significantly upregulated in both centre and margin microdissected KE and Kd. This molecule has been linked to both overexpression of *ErbB2* [158, 159], which we found upregulated in margin Kd ($p = 0.0031$) and loss of *PTEN* [160, 161], which was also significantly downregulated in the margin Kd in our microarray data ($p = 2.86 \times 10^{-5}$). *TUBB3* is associated with aggressive tumorigenesis in hypoxic environments [162], where it has been linked with chemoresistance, particularly taxanes [163–165]. This may be relevant to KD where there is evidence of a similarly hypoxic environment [63, 166, 167].

KD is notoriously difficult to manage in the clinical setting, with several available treatments but no one absolutely effective therapy [168–170]. Drug resistance has formed a major part of this failure [171]. In identifying DEG that may contribute to this seemingly multi-drug-resistant disease, it may be possible to tailor management by targeting these molecules with adjuvant therapies.

Microarray data was validated through qRT-PCR of interesting targets

We chose four candidate genes from each of the KE and Kd for qRT-PCR validation of the microarray findings. For the epidermis, the dysregulation of *AKR1B10* and associated *AKR1B1*, *AKR1B15* and *ALDH1A1* all related to the retinoic acid pathway and as such were previously validated [23]. Also in the KE, we wanted to validate genes representing different areas of interest including epidermal activation and inflammation (*CD36*), EMT (*WDR66* and

BMP2) and the possible existence of a cancer-like stem cell population (*NOTCH4*). As the most abundant protein in keloid ECM, collagen has long been investigated as a potential therapeutic target. Our identification of *ADAMTS14*, *ADAMTS2*, *COMP* and *ADAM12* represent significant alternative targets to *TGF*β and as such were chosen for validation in the dermis. qRT-PCR for these genes not only reflected the microarray findings but also preserved the site-specific differences in expression, thus validating our data (**Fig 7**).

Conclusions and perspectives

In this study, we have combined LCM and microarray to examine KD by looking at the lesion as separate components; epidermis and dermis as well as centre, margin and extralesional sites. First, we showed this *in situ* microdissection approach was both more accurate and more sensitive than either whole tissue biopsy or monolayer cell culture methods in the dissection of the heterogeneous lesion that is keloid scar.

Through this strategy, we have distinguished several genes that are either novel or supportive of emerging literature with respect to KD pathobiology. In this study, expression patterns indicate the possible residence of a cancer-like stem cell population in KD, an area that is surprisingly under-researched in this field given the association with both EMT and drug resistance [171, 172]. The plausible presence of such a cell population in KD, which to date has been associated with an inflammatory infiltrate [13, 34, 128], provides a reasonable explanation for the persistent growth, recurrence and multi-drug resistance that are characteristic of this disorder. The LCM strategy detailed in this study could benefit the isolation and characterisation of these cancer-like stem cells from within the keloid tissue and therefore constitutes an interesting focus for future work.

The multi-level ECM regulators, *ADAMTS14* and *ADAMTS2*, make attractive KD therapeutic targets. The potential redundancy of both these proteins with *ADAMTS3*, which we did not find to be upregulated in KD, indicates possible attenuation of their effect without the consequences of complete abrogation. *IL-37* overexpression *in vivo* in transgenic mice has resulted in dampened *IL-6*, *IL-1*β and *IL-17* [173], which are all previously shown to be upregulated in KD [13]. This suggests therapeutic induction of IL-37 expression in KE, in order to dampen the pathologic inflammatory response, may be a prospective management strategy. Interestingly, there is differential gene expression between extralesional keloid and NS tissue. This may represent a field cancerisation effect whereby keloid tumour invasive growth is mediated by paracrine signalling with the adjacent NS and that within this extralesional perimeter the risk of keloid recurrence following treatment is greatest. Therefore, establishment of the extent of this extralesional expression divergence from that of NS may have clinical implications for future management of KD.

Given the clinically distinct keloid phenotypes and the morphological heterogeneity within the keloid scar, which is fully reflected here by the isolated gene expression profile of defined KD-associated lesion compartments, it is most likely a gene signature rather than a single biomarker that will prove valuable as a diagnostic tool when distinguishing KD from other cutaneous fibroses. Improved differential diagnosis prevents the morbidity and mortality associated with inappropriate management of clinically comparable conditions, some of which may have more serious consequences if improperly treated (for example; dermatofibrosarcoma protuberans and systemic sclerosis). The heterogeneity of KD has been addressed through the innovative microdissection gene expression profiling approach in this study, which has provided a better-defined gene signature of distinct regions of keloid tissue pathobiology (**Fig 8**).

It is likely that the complex nature of KD results from an interplay of simultaneously occurring processes, such that injury to the epidermis results in inflammation which then through

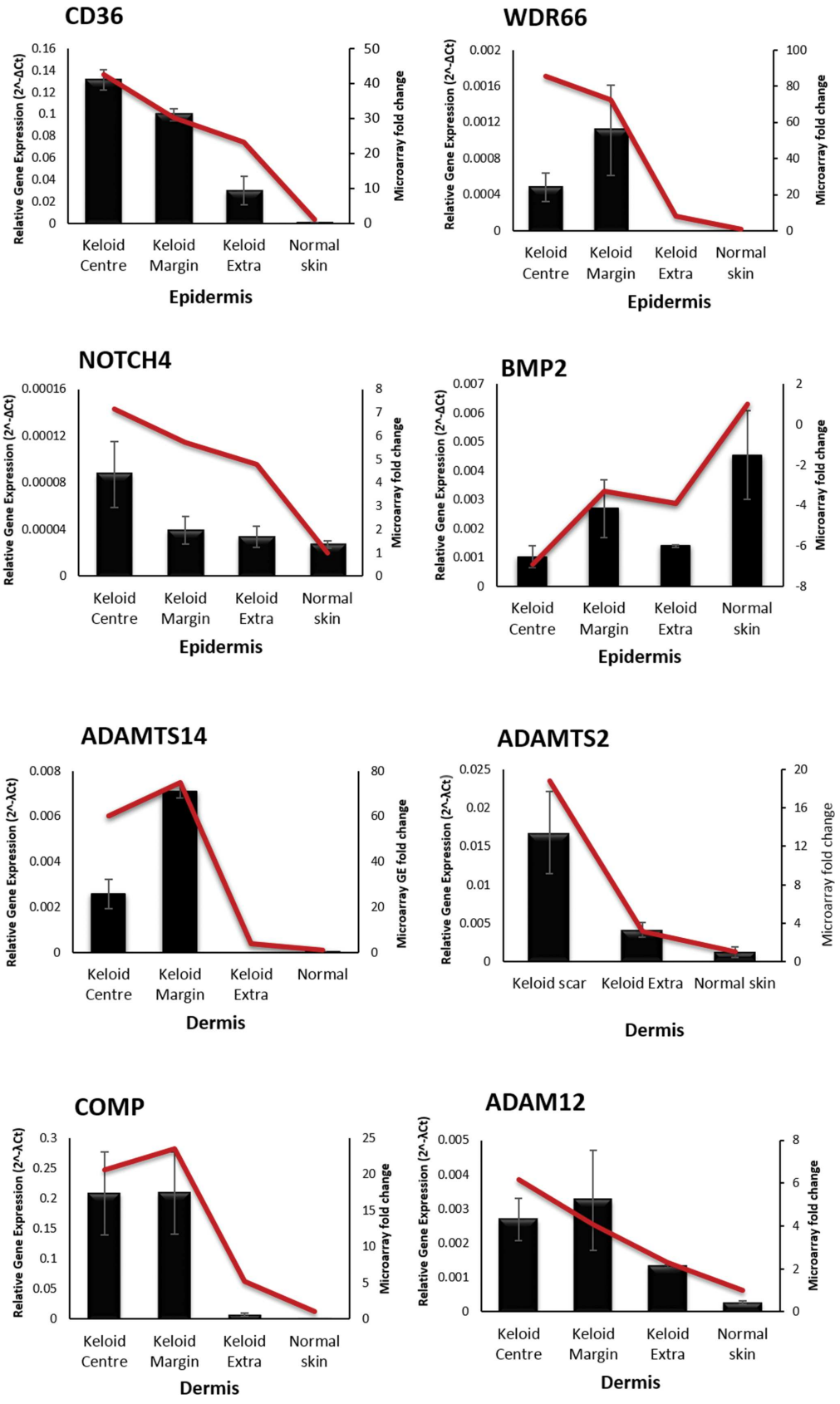
CD36
Relative Gene Expression (2^-ΔCt)
Microarray fold change
Keloid Centre
Keloid Margin
Keloid Extra
Normal skin
Epidermis
WDR66
Relative Gene Expression (2^-ΔCt)
Microarray fold change
Keloid Centre
Keloid Margin
Keloid Extra
Normal skin
Epidermis
NOTCH4
Relative Gene Expression (2^-ΔCt)
Microarray fold change
Keloid Centre
Keloid Margin
Keloid Extra
Normal skin
Epidermis
BMP2
Relative Gene Expression (2^-ΔCt)
Microarray fold change
Keloid Centre
Keloid Margin
Keloid Extra
Normal skin
Epidermis
ADAMTS14
Relative Gene Expression (2^-λCt)
Microarray GE fold change
Keloid Centre
Keloid Margin
Keloid Extra
Normal
Dermis
ADAMTS2
Relative Gene Expression (2^-λCt)
Microarray fold change
Keloid scar
Keloid Extra
Normal skin
Dermis
COMP
Relative Gene Expression (2^-λCt)
Microarray fold change
Keloid Centre
Keloid Margin
Keloid Extra
Normal skin
Dermis
ADAM12
Relative Gene Expression (2^-λCt)
Microarray fold change
Keloid Centre
Keloid Margin
Keloid Extra
Normal skin
Dermis

Fig 7. qRT-PCR validation of candidate genes. Four candidate genes were chosen from each of the epidermis and dermis for validation by qRT-PCR. The bar graphs represent the qRT-PCR data for the microdissected keloid sites and normal skin and the line graph represents the associated microarray fold change in gene expression. In all cases the line graph follows the trend of the bar graph indicating the PCR reflects the microarray, thus validating the data. Data are presented as mean ± SEM and are from at least three independent experiments. For some of the genes there was no expression in normal skin and therefore for those genes no fold change for the qRT-PCR could be generated. In the interest of standardisation of all of the graphs they were then presented with the two axes. ADAM, a disintegrin and metalloproteinase; ADAMTS, a disintegrin and metalloproteinase with thrombospondin motifs; BMP2, bone morphogenetic protein 2; CD36, cluster of differentiation 36; COMP, cartilage oligomeric protein; NOTCH4, notch 4; WDR66, WD repeat domain 66.

doi:10.1371/journal.pone.0172955.g007

autocrine and paracrine signalling recruits factors that trigger EMT, which in turn can trigger cellular reversion to a stem cell-like state and thus exacerbate drug resistance and recurrence [174]. While *TGF*β is an attractive therapeutic target, the pleiotropic nature of this molecule makes a simplistic TGFβ-neutralisation strategy imprudent. Therefore, it would be useful if alternative molecular mechanisms that are important in KD pathobiology but more specific to it, could be selectively targeted therapeutically. Several novel, potentially important molecular targets and KD pathobiology candidate mechanisms have been dissected here that invite and facilitate further studies. To this end, the use of LCM in this study is in keeping with previous research that highlighted the superiority of this technique with regard to identification of otherwise overlooked genes using traditional methods as well as an increased number of genes reaching significance [175–178]. Our approach therefore offers a competitive alternative to established methods of experimentation and may be of potential benefit not only to KD but also other heterogeneous conditions.

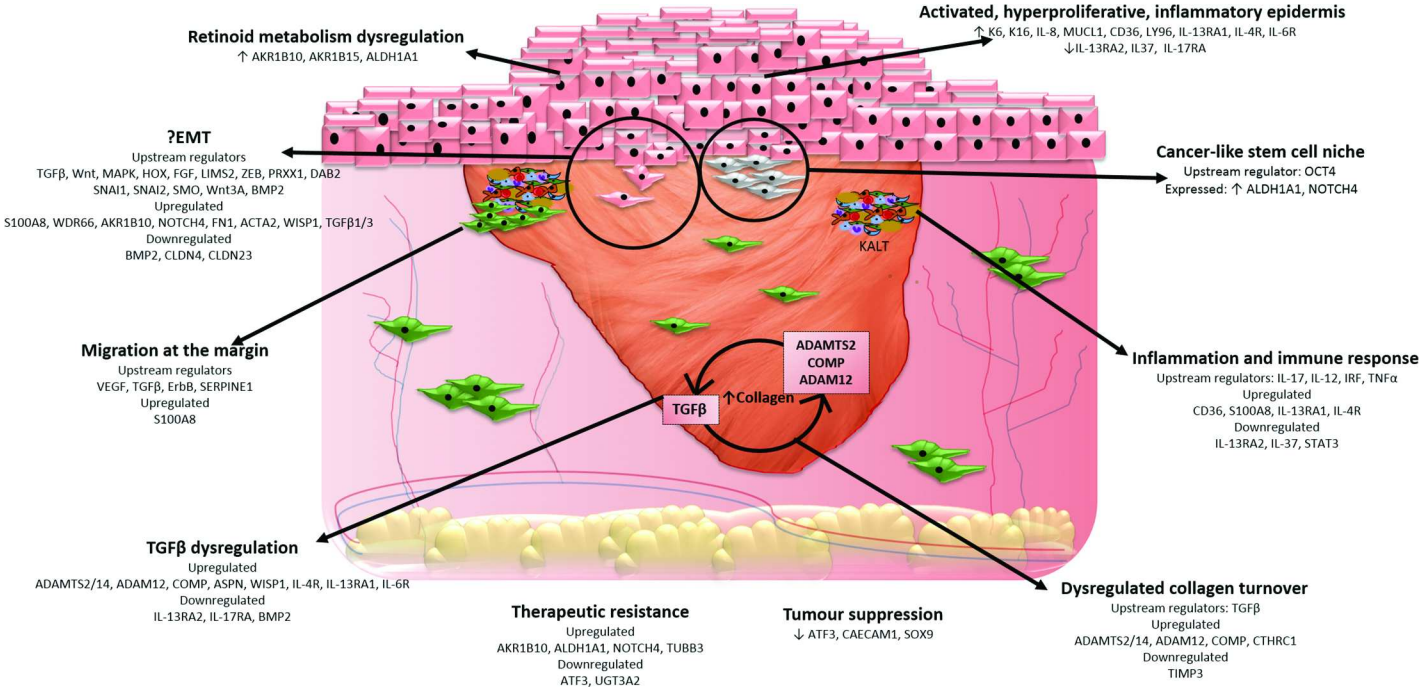

Fig 8. Summary figure of proposed processes and mechanisms contributing to keloid disease based on identification of DEG and subsequent analysis.

doi:10.1371/journal.pone.0172955.g008

Supporting information

S1 Table. Demographic data for the samples used in this study.
(DOCX)

S2 Table. Expanded names for each of the gene symbols used throughout the manuscript text and figures.
(DOCX)

S1 Fig. Correlated modules based on assessment of eigengene plots.
(DOCX)

S2 Fig. qRT-PCR comparing LCM and monolayer and defining site-specific contribution to gene expression.
(DOCX)

S3 Fig. Top upregulated genes in keloid vs normal skin epidermis.
(DOCX)

S4 Fig. Top downregulated genes in keloid vs normal skin epidermis.
(DOCX)

S5 Fig. Top 100 upregulated genes in keloid centre vs normal skin epidermis.
(DOCX)

S6 Fig. Top 50 downregulated genes in keloid centre vs normal skin epidermis.
(DOCX)

S7 Fig. Top 100 upregulated genes in keloid margin vs normal skin epidermis.
(DOCX)

S8 Fig. Top 50 downregulated genes in keloid margin vs normal skin epidermis.
(DOCX)

S9 Fig. Top 100 upregulated genes in keloid extralesional vs normal skin epidermis.
(DOCX)

S10 Fig. Top 50 downregulated genes in keloid extralesional vs normal skin epidermis.
(DOCX)

S11 Fig. Top 100 upregulated genes in keloid centre vs normal skin dermis.
(DOCX)

S12 Fig. Top 50 downregulated genes in keloid centre vs normal skin dermis.
(DOCX)

S13 Fig. Top 100 upregulated genes in keloid margin vs normal skin dermis.
(DOCX)

S14 Fig. Top 50 downregulated genes in keloid margin vs normal skin dermis.
(DOCX)

S15 Fig. Top 100 upregulated genes in keloid extralesional vs normal skin dermis.
(DOCX)

S16 Fig. Top 50 downregulated genes in keloid extralesional vs normal skin dermis.
(DOCX)

Acknowledgments

The authors are grateful to Yaron Har-Shai and Guyan Arscott for their assistance with tissue sample provision and particularly to Adam Taylor for his contribution to the microarray analysis. We thank Leo Zeef of the Bioinformatics and Genomic Technologies Core Facilities at the University of Manchester for providing support with regard to microarray accession.

Author Contributions

Conceptualization: NJ RP AB.

Data curation: NJ AB.

Formal analysis: NJ.

Funding acquisition: AB.

Investigation: NJ TH.

Methodology: NJ TH RP AB.

Project administration: NJ AB.

Resources: NJ AB.

Supervision: RP AB.

Validation: NJ TH.

Visualization: NJ TH RP AB.

Writing – original draft: NJ AB.

Writing – review & editing: NJ TH RP AB.

References

1. Jumper N, Paus R, Bayat A. Functional histopathology of keloid disease. Histol Histopathol. 2015; 30: 1033–57. doi: 10.14670/HH-11-624 PMID: 25900252
2. Berman B, Kaufman J. Pilot study of the effect of postoperative imiquimod 5% cream on the recurrence rate of excised keloids. Journal of the American Academy of Dermatology. 2002; 47: S209–11. PMID: 12271279
3. Marttala J, Andrews JP, Rosenbloom J, Uitto J. Keloids: Animal models and pathologic equivalents to study tissue fibrosis. Matrix Biol. 2016.
4. Butler PD, Longaker MT, Yang GP. Current progress in keloid research and treatment. J Am Coll Surg. 2008; 206: 731–41. doi: 10.1016/j.jamcollsurg.2007.12.001 PMID: 18387480
5. Seifert O, Bayat A, Geffers R, Dienus K, Buer J, Lofgren S, et al. Identification of unique gene expression patterns within different lesional sites of keloids. Wound repair and regeneration: official publication of the Wound Healing Society [and] the European Tissue Repair Society. 2008; 16: 254–65.
6. Bagabir R, Byers RJ, Chaudhry IH, Muller W, Paus R, Bayat A. Site-specific immunophenotyping of keloid disease demonstrates immune upregulation and the presence of lymphoid aggregates. Br J Dermatol. 2012; 167: 1053–66. doi: 10.1111/j.1365-2133.2012.11190.x PMID: 23106354
7. Syed F, Ahmadi E, Iqbal SA, Singh S, McGrouther DA, Bayat A. Fibroblasts from the growing margin of keloid scars produce higher levels of collagen I and III compared with intralesional and extralesional sites: clinical implications for lesional site-directed therapy. Br J Dermatol. 2011; 164: 83–96. doi: 10.1111/j.1365-2133.2010.10048.x PMID: 20849516
8. Lu F, Gao J, Ogawa R, Hyakusoku H, Ou C. Biological differences between fibroblasts derived from peripheral and central areas of keloid tissues. Plast Reconstr Surg. 2007; 120: 625–30. doi: 10.1097/01.prs.0000270293.93612.7b PMID: 17700113
9. Mitsui H, Suarez-Farinas M, Belkin DA, Levenkova N, Fuentes-Duculan J, Coats I, et al. Combined use of laser capture microdissection and cDNA microarray analysis identifies locally expressed

disease-related genes in focal regions of psoriasis vulgaris skin lesions. The Journal of investigative dermatology. 2012; 132: 1615–26. doi: 10.1038/jid.2012.33 PMID: 22402443

10. Marmai C, Sutherland RE, Kim KK, Dolganov GM, Fang X, Kim SS, et al. Alveolar epithelial cells express mesenchymal proteins in patients with idiopathic pulmonary fibrosis. Am J Physiol Lung Cell Mol Physiol. 2011; 301: L71–8. doi: 10.1152/ajplung.00212.2010 PMID: 21498628
11. Makhzami S, Rambow F, Delmas V, Larue L. Efficient gene expression profiling of laser-microdissected melanoma metastases. Pigment Cell Melanoma Res. 2012; 25: 783–91. doi: 10.1111/pcmr.12013 PMID: 22934821
12. Mabry KM, Payne SZ, Anseth KS. Microarray analyses to quantify advantages of 2D and 3D hydrogel culture systems in maintaining the native valvular interstitial cell phenotype. Biomaterials. 2016; 74: 31–41. doi: 10.1016/j.biomaterials.2015.09.035 PMID: 26433490
13. Zhang Q, Yamaza T, Kelly AP, Shi S, Wang S, Brown J, et al. Tumor-like stem cells derived from human keloid are governed by the inflammatory niche driven by IL-17/IL-6 axis. PLoS One. 2009; 4: e7798. doi: 10.1371/journal.pone.0007798 PMID: 19907660
14. Lee JY, Yang CC, Chao SC, Wong TW. Histopathological differential diagnosis of keloid and hypertrophic scar. Am J Dermatopathol. 2004; 26: 379–84. PMID: 15365369
15. Bayat A, Arscott G, Ollier WE, McGrouther DA, Ferguson MW. Keloid disease: clinical relevance of single versus multiple site scars. British journal of plastic surgery. 2005; 58: 28–37. doi: 10.1016/j.bjps.2004.04.024 PMID: 15629164
16. Clement-Ziza M, Munnich A, Lyonnet S, Jaubert F, Besmond C. Stabilization of RNA during laser capture microdissection by performing experiments under argon atmosphere or using ethanol as a solvent in staining solutions. RNA. 2008; 14: 2698–704. doi: 10.1261/rna.1261708 PMID: 18945804
17. Kolijn K, van Leenders GJ. Comparison of RNA extraction kits and histological stains for laser capture microdissected prostate tissue. BMC research notes. 2016; 9: 1–6.
18. Harries MJ, Meyer K, Chaudhry I, J EK, Poblet E, Griffiths CE, et al. Lichen planopilaris is characterized by immune privilege collapse of the hair follicle's epithelial stem cell niche. J Pathol. 2013; 231: 236–47. doi: 10.1002/path.4233 PMID: 23788005
19. Kameda T, Shide K, Yamaji T, Kamiunten A, Sekine M, Hidaka T, et al. Gene expression profiling of loss of TET2 and/or JAK2V617F mutant hematopoietic stem cells from mouse models of myeloproliferative neoplasms. Genomics data. 2015; 4: 102–8. doi: 10.1016/j.gdata.2015.04.002 PMID: 26484191
20. Masuda A, Katoh N, Nakabayashi K, Kato K, Sonoda K, Kitade M, et al. An improved method for isolation of epithelial and stromal cells from the human endometrium. The Journal of reproduction and development. 2016; 62: 213. doi: 10.1262/jrd.2015-137 PMID: 26853786
21. Leguen I, Le Cam A, Montfort J, Peron S, Fautrel A. Transcriptomic Analysis of Trout Gill Ionocytes in Fresh Water and Sea Water Using Laser Capture Microdissection Combined with Microarray Analysis. PloS one. 2015; 10: e0139938. doi: 10.1371/journal.pone.0139938 PMID: 26439495
22. Ashcroft KJ, Syed F, Bayat A. Site-specific keloid fibroblasts alter the behaviour of normal skin and normal scar fibroblasts through paracrine signalling. PLoS One. 2013; 8: e75600. doi: 10.1371/journal.pone.0075600 PMID: 24348987
23. Jumper N, Hodgkinson T, Arscott G, Har-Shai Y, Paus R, Bayat A. The aldo-keto reductase AKR1B10 is upregulated in keloid epidermis, implicating retinoic acid pathway dysregulation in the pathogenesis of keloid disease. The Journal of investigative dermatology. 2016 Jul; 136(7):1500–12. doi: 10.1016/j.jid.2016.03.022 PMID: 27025872
24. Benjamini Y, Hochberg Y. Controlling the false discovery rate: a practical and powerful approach to multiple testing. Journal of the royal statistical society Series B (Methodological). 1995: 289–300.
25. Sidgwick GP, McGeorge D, Bayat A. Functional testing of topical skin formulations using an optimised ex vivo skin organ culture model. Arch Dermatol Res. 2016; 308: 297–308. doi: 10.1007/s00403-016-1645-8 PMID: 27086034
26. Bolstad BM, Irizarry RA, Åstrand M, Speed TP. A comparison of normalization methods for high density oligonucleotide array data based on variance and bias. Bioinformatics. 2003; 19: 185–93. PMID: 12538238
27. Ringnér M. What is principal component analysis? Nature biotechnology. 2008; 26: 303–4. doi: 10.1038/nbt0308-303 PMID: 18327243
28. Oliveros J. Venny. An interactive tool for comparing lists with Venn's diagrams.(2007–2015).
29. Baker BM, Chen CS. Deconstructing the third dimension: how 3D culture microenvironments alter cellular cues. J Cell Sci. 2012; 125: 3015–24. doi: 10.1242/jcs.079509 PMID: 22797912

30. Lee WJ, Park JH, Shin JU, Noh H, Lew DH, Yang WI, et al. Endothelial-to-mesenchymal transition induced by Wnt 3a in keloid pathogenesis. Wound repair and regeneration: official publication of the Wound Healing Society [and] the European Tissue Repair Society. 2015; 23: 435–42.

31. Lamouille S, Xu J, Derynck R. Molecular mechanisms of epithelial-mesenchymal transition. Nat Rev Mol Cell Biol. 2014; 15: 178–96. doi: 10.1038/nrm3758 PMID: 24556840

32. Yang YL, Ju HZ, Liu SF, Lee TC, Shih YW, Chuang LY, et al. BMP-2 suppresses renal interstitial fibrosis by regulating epithelial-mesenchymal transition. J Cell Biochem. 2011; 112: 2558–65. doi: 10.1002/jcb.23180 PMID: 21590708

33. Pratap A, Singh S, Mundra V, Yang N, Panakanti R, Eason JD, et al. Attenuation of early liver fibrosis by pharmacological inhibition of smoothened receptor signaling. J Drug Target. 2012; 20: 770–82. doi: 10.3109/1061186X.2012.719900 PMID: 22994359

34. Grant C, Chudakova DA, Itinteang T, Chibnall AM, Brasch HD, Davis PF, et al. Expression of embryonic stem cell markers in keloid-associated lymphoid tissue. J Clin Pathol. 2016.

35. Honda K, Yanai H, Negishi H, Asagiri M, Sato M, Mizutani T, et al. IRF-7 is the master regulator of type-I interferon-dependent immune responses. Nature. 2005; 434: 772–7. doi: 10.1038/nature03464 PMID: 15800576

36. Lu P, Weaver VM, Werb Z. The extracellular matrix: a dynamic niche in cancer progression. J Cell Biol. 2012; 196: 395–406. doi: 10.1083/jcb.201102147 PMID: 22351925

37. Pan X, Hobbs RP, Coulombe PA. The expanding significance of keratin intermediate filaments in normal and diseased epithelia. Curr Opin Cell Biol. 2013; 25: 47–56. doi: 10.1016/j.ceb.2012.10.018 PMID: 23270662

38. Rotty JD, Coulombe PA. A wound-induced keratin inhibits Src activity during keratinocyte migration and tissue repair. J Cell Biol. 2012; 197: 381–9. doi: 10.1083/jcb.201107078 PMID: 22529101

39. Luo S, Yufit T, Carson P, Fiore D, Falanga J, Lin X, et al. Differential keratin expression during epiboly in a wound model of bioengineered skin and in human chronic wounds. Int J Low Extrem Wounds. 2011; 10: 122–9. doi: 10.1177/1534734611418157 PMID: 21856973

40. Leigh IM, Navsaria H, Purkis PE, McKay IA, Bowden PE, Riddle PN. Keratins (K16 and K17) as markers of keratinocyte hyperproliferation in psoriasis in vivo and in vitro. Br J Dermatol. 1995; 133: 501–11. PMID: 7577575

41. Conley SJ, Bosco EE, Tice DA, Hollingsworth RE, Herbst R, Xiao Z. HER2 drives Mucin-like 1 to control proliferation in breast cancer cells. Oncogene. 2016.

42. Hakvoort TE, Altun V, Ramrattan RS, van der Kwast TH, Benner R, van Zuijlen PP, et al. Epidermal participation in post-burn hypertrophic scar development. Virchows Arch. 1999; 434: 221–6. PMID: 10190301

43. Santucci M, Borgognoni L, Reali UM, Gabbiani G. Keloids and hypertrophic scars of Caucasians show distinctive morphologic and immunophenotypic profiles. Virchows Arch. 2001; 438: 457–63. PMID: 11407473

44. Alessio M, Gruarin P, Castagnoli C, Trombotto C, Stella M. Primary ex vivo culture of keratinocytes isolated from hypertrophic scars as a means of biochemical characterization of CD36. Int J Clin Lab Res. 1998; 28: 47–54. PMID: 9594363

45. Xiong W, Frasch SC, Thomas SM, Bratton DL, Henson PM. Induction of TGF-beta1 synthesis by macrophages in response to apoptotic cells requires activation of the scavenger receptor CD36. PLoS One. 2013; 8: e72772. doi: 10.1371/journal.pone.0072772 PMID: 23936544

46. He S, Liu X, Yang Y, Huang W, Xu S, Yang S, et al. Mechanisms of transforming growth factor beta(1)/Smad signalling mediated by mitogen-activated protein kinase pathways in keloid fibroblasts. Br J Dermatol. 2010; 162: 538–46. doi: 10.1111/j.1365-2133.2009.09511.x PMID: 19772524

47. Zhou P, Shi L, Li Q, Lu D. Overexpression of RACK1 inhibits collagen synthesis in keloid fibroblasts via inhibition of transforming growth factor-beta1/Smad signaling pathway. Int J Clin Exp Med. 2015; 8: 15262–8. PMID: 26629012

48. Zhong A, Xu W, Zhao J, Xie P, Jia S, Sun J, et al. S100A8 and S100A9 Are Induced by Decreased Hydration in the Epidermis and Promote Fibroblast Activation and Fibrosis in the Dermis. Am J Pathol. 2016; 186: 109–22. doi: 10.1016/j.ajpath.2015.09.005 PMID: 26597884

49. Ryckman C, Vandal K, Rouleau P, Talbot M, Tessier PA. Proinflammatory activities of S100: proteins S100A8, S100A9, and S100A8/A9 induce neutrophil chemotaxis and adhesion. The Journal of Immunology. 2003; 170: 3233–42. PMID: 12626582

50. Ong C, Khoo Y, Mukhopadhyay A, Masilamani J, Do D, Lim I, et al. Comparative proteomic analysis between normal skin and keloid scar. British Journal of Dermatology. 2010; 162: 1302–15. doi: 10.1111/j.1365-2133.2010.09660.x PMID: 20128793

51. Kerkhoff C, Voss A, Scholzen TE, Averill MM, Zänker KS, Bornfeldt KE. Novel insights into the role of S100A8/A9 in skin biology. Experimental dermatology. 2012; 21: 822–6. doi: 10.1111/j.1600-0625.2012.01571.x PMID: 22882537

52. Wang Q, Ma C, Kemmner W. Wdr66 is a novel marker for risk stratification and involved in epithelial-mesenchymal transition of esophageal squamous cell carcinoma. BMC Cancer. 2013; 13: 137. doi: 10.1186/1471-2407-13-137 PMID: 23514407

53. Kalluri R, Neilson EG. Epithelial-mesenchymal transition and its implications for fibrosis. J Clin Invest. 2003; 112: 1776–84. doi: 10.1172/JCI20530 PMID: 14679171

54. Thiery JP, Sleeman JP. Complex networks orchestrate epithelial-mesenchymal transitions. Nat Rev Mol Cell Biol. 2006; 7: 131–42. doi: 10.1038/nrm1835 PMID: 16493418

55. Hahn JM, Glaser K, McFarland KL, Aronow BJ, Boyce ST, Supp DM. Keloid-derived keratinocytes exhibit an abnormal gene expression profile consistent with a distinct causal role in keloid pathology. Wound repair and regeneration: official publication of the Wound Healing Society [and] the European Tissue Repair Society. 2013; 21: 530–44.

56. Do DV, Ong CT, Khoo YT, Carbone A, Lim CP, Wang S, et al. Interleukin-18 system plays an important role in keloid pathogenesis via epithelial-mesenchymal interactions. Br J Dermatol. 2012; 166: 1275–88. doi: 10.1111/j.1365-2133.2011.10721.x PMID: 22050194

57. Shang X, Lin X, Alvarez E, Manorek G, Howell SB. Tight junction proteins claudin-3 and claudin-4 control tumor growth and metastases. Neoplasia. 2012; 14: 974–IN22. PMID: 23097631

58. Lin X, Shang X, Manorek G, Howell SB. Regulation of the Epithelial-Mesenchymal Transition by Claudin-3 and Claudin-4. PLoS One. 2013; 8: e67496. doi: 10.1371/journal.pone.0067496 PMID: 23805314

59. Michl P, Barth C, Buchholz M, Lerch MM, Rolke M, Holzmann KH, et al. Claudin-4 expression decreases invasiveness and metastatic potential of pancreatic cancer. Cancer Res. 2003; 63: 6265–71. PMID: 14559813

60. Bujko M, Kober P, Mikula M, Ligaj M, Ostrowski J, Siedlecki JA. Expression changes of cell-cell adhesion-related genes in colorectal tumors. Oncol Lett. 2015; 9: 2463–70. doi: 10.3892/ol.2015.3107 PMID: 26137091

61. Harrison H, Farnie G, Howell SJ, Rock RE, Stylianou S, Brennan KR, et al. Regulation of breast cancer stem cell activity by signaling through the Notch4 receptor. Cancer Res. 2010; 70: 709–18. doi: 10.1158/0008-5472.CAN-09-1681 PMID: 20068161

62. Bonyadi Rad E, Hammerlindl H, Wels C, Popper U, Ravindran Menon D, Breiteneder H, et al. Notch4 Signaling Induces a Mesenchymal-Epithelial-like Transition in Melanoma Cells to Suppress Malignant Behaviors. Cancer Res. 2016.

63. Ma X, Chen J, Xu B, Long X, Qin H, Zhao RC, et al. Keloid-derived keratinocytes acquire a fibroblast-like appearance and an enhanced invasive capacity in a hypoxic microenvironment in vitro. Int J Mol Med. 2015; 35: 1246–56. doi: 10.3892/ijmm.2015.2135 PMID: 25777304

64. Yan L, Cao R, Wang L, Liu Y, Pan B, Yin Y, et al. Epithelial-mesenchymal transition in keloid tissues and TGF-beta1-induced hair follicle outer root sheath keratinocytes. Wound repair and regeneration: official publication of the Wound Healing Society [and] the European Tissue Repair Society. 2015; 23: 601–10.

65. Kalluri R, Weinberg RA. The basics of epithelial-mesenchymal transition. The Journal of clinical investigation. 2009; 119: 1420–8. doi: 10.1172/JCI39104 PMID: 19487818

66. Verrecchia F, Mauviel A. Transforming growth factor-beta and fibrosis. World J Gastroenterol. 2007; 13: 3056–62. doi: 10.3748/wjg.v13.i22.3056 PMID: 17589920

67. Lan CC, Fang AH, Wu PH, Wu CS. Tacrolimus abrogates TGF-beta1-induced type I collagen production in normal human fibroblasts through suppressing p38MAPK signalling pathway: implications on treatment of chronic atopic dermatitis lesions. J Eur Acad Dermatol Venereol. 2014; 28: 204–15. doi: 10.1111/jdv.12086 PMID: 23301526

68. Steplewski A, Fertala A. Inhibition of collagen fibril formation. Fibrogenesis Tissue Repair. 2012; 5: S29. doi: 10.1186/1755-1536-5-S1-S29 PMID: 23259659

69. Kelwick R, Desanlis I, Wheeler GN, Edwards DR. The ADAMTS (A Disintegrin and Metalloproteinase with Thrombospondin motifs) family. Genome Biol. 2015; 16: 113. doi: 10.1186/s13059-015-0676-3 PMID: 26025392

70. Bekhouche M, Colige A. The procollagen N-proteinases ADAMTS2, 3 and 14 in pathophysiology. Matrix Biol. 2015; 44–46: 46–53. doi: 10.1016/j.matbio.2015.04.001 PMID: 25863161

71. Colige A, Vandenberghe I, Thiry M, Lambert CA, Van Beeumen J, Li SW, et al. Cloning and characterization of ADAMTS-14, a novel ADAMTS displaying high homology with ADAMTS-2 and ADAMTS-3.

The Journal of biological chemistry. 2002; 277: 5756–66. doi: 10.1074/jbc.M105601200 PMID: 11741898

72. Broder C, Arnold P, Vadon-Le Goff S, Konerding MA, Bahr K, Muller S, et al. Metalloproteases meprin alpha and meprin beta are C- and N-procollagen proteinases important for collagen assembly and tensile strength. Proc Natl Acad Sci U S A. 2013; 110: 14219–24. doi: 10.1073/pnas.1305464110 PMID: 23940311

73. Johnston P, Chojnowski AJ, Davidson RK, Riley GP, Donell ST, Clark IM. A complete expression profile of matrix-degrading metalloproteinases in Dupuytren's disease. J Hand Surg Am. 2007; 32: 343–51. doi: 10.1016/j.jhsa.2006.12.010 PMID: 17336841

74. Zhou SH, Yang WJ, Liu SW, Li J, Zhang CY, Zhu Y, et al. Gene expression profiling of craniofacial fibrous dysplasia reveals ADAMTS2 overexpression as a potential marker. Int J Clin Exp Pathol. 2014; 7: 8532–41. PMID: 25674217

75. Colige A, Nuytinck L, Hausser I, van Essen AJ, Thiry M, Herens C, et al. Novel types of mutation responsible for the dermatosparactic type of Ehlers-Danlos syndrome (Type VIIC) and common polymorphisms in the ADAMTS2 gene. The Journal of investigative dermatology. 2004; 123: 656–63. doi: 10.1111/j.0022-202X.2004.23406.x PMID: 15373769

76. Kumar S, Rao N, Ge R. Emerging Roles of ADAMTSs in Angiogenesis and Cancer. Cancers (Basel). 2012; 4: 1252–99.

77. Cal S, Lopez-Otin C. ADAMTS proteases and cancer. Matrix Biol. 2015; 44–46: 77–85. doi: 10.1016/j.matbio.2015.01.013 PMID: 25636539

78. Li SW, Arita M, Fertala A, Bao Y, Kopen GC, Langsjo TK, et al. Transgenic mice with inactive alleles for procollagen N-proteinase (ADAMTS-2) develop fragile skin and male sterility. Biochem J. 2001; 355: 271–8. PMID: 11284712

79. Kesteloot F, Desmouliere A, Leclercq I, Thiry M, Arrese JE, Prockop DJ, et al. ADAM metallopeptidase with thrombospondin type 1 motif 2 inactivation reduces the extent and stability of carbon tetrachloride-induced hepatic fibrosis in mice. Hepatology. 2007; 46: 1620–31. doi: 10.1002/hep.21868 PMID: 17929299

80. Wang WM, Lee S, Steiglitz BM, Scott IC, Lebares CC, Allen ML, et al. Transforming growth factor-beta induces secretion of activated ADAMTS-2. A procollagen III N-proteinase. The Journal of biological chemistry. 2003; 278: 19549–57. doi: 10.1074/jbc.M300767200 PMID: 12646579

81. Bekhouche M, Leduc C, Dupont L, Janssen L, Delolme F, Vadon-Le Goff S, et al. Determination of the substrate repertoire of ADAMTS2, 3, and 14 significantly broadens their functions and identifies extracellular matrix organization and TGF-beta signaling as primary targets. FASEB J. 2016.

82. Jones GC, Riley GP. ADAMTS proteinases: a multi-domain, multi-functional family with roles in extracellular matrix turnover and arthritis. Arthritis Res Ther. 2005; 7: 160–9. doi: 10.1186/ar1783 PMID: 15987500

83. Wang WM, Ge G, Lim NH, Nagase H, Greenspan DS. TIMP-3 inhibits the procollagen N-proteinase ADAMTS-2. Biochem J. 2006; 398: 515–9. doi: 10.1042/BJ20060630 PMID: 16771712

84. Dulauroy S, Di Carlo SE, Langa F, Eberl G, Peduto L. Lineage tracing and genetic ablation of ADAM12 (+) perivascular cells identify a major source of profibrotic cells during acute tissue injury. Nat Med. 2012; 18: 1262–70. doi: 10.1038/nm.2848 PMID: 22842476

85. Shih B, Wijeratne D, Armstrong DJ, Lindau T, Day P, Bayat A. Identification of biomarkers in Dupuytren's disease by comparative analysis of fibroblasts versus tissue biopsies in disease-specific phenotypes. J Hand Surg Am. 2009; 34: 124–36. doi: 10.1016/j.jhsa.2008.09.017 PMID: 19121738

86. Kveiborg M, Albrechtsen R, Couchman JR, Wewer UM. Cellular roles of ADAM12 in health and disease. The international journal of biochemistry & cell biology. 2008; 40: 1685–702.

87. Ruff M, Leyme A, Le Cann F, Bonnier D, Le Seyec J, Chesnel F, et al. The Disintegrin and Metalloprotease ADAM12 Is Associated with TGF-beta-Induced Epithelial to Mesenchymal Transition. PLoS One. 2015; 10: e0139179. doi: 10.1371/journal.pone.0139179 PMID: 26407179

88. Naitoh M, Kubota H, Ikeda M, Tanaka T, Shirane H, Suzuki S, et al. Gene expression in human keloids is altered from dermal to chondrocytic and osteogenic lineage. Genes Cells. 2005; 10: 1081–91. doi: 10.1111/j.1365-2443.2005.00902.x PMID: 16236136

89. Inui S, Shono F, Nakajima T, Hosokawa K, Itami S. Identification and characterization of cartilage oligomeric matrix protein as a novel pathogenic factor in keloids. Am J Pathol. 2011; 179: 1951–60. doi: 10.1016/j.ajpath.2011.06.034 PMID: 21872564

90. Agarwal P, Schulz JN, Blumbach K, Andreasson K, Heinegard D, Paulsson M, et al. Enhanced deposition of cartilage oligomeric matrix protein is a common feature in fibrotic skin pathologies. Matrix Biol. 2013; 32: 325–31. doi: 10.1016/j.matbio.2013.02.010 PMID: 23507196

91. Li J, Cao J, Li M, Yu Y, Yang Y, Xiao X, et al. Collagen triple helix repeat containing-1 inhibits transforming growth factor-b1-induced collagen type I expression in keloid. Br J Dermatol. 2011; 164: 1030–6. PMID: 21667528

92. Bauer Y, Tedrow J, de Bernard S, Birker-Robaczewska M, Gibson KF, Guardela BJ, et al. A novel genomic signature with translational significance for human idiopathic pulmonary fibrosis. Am J Respir Cell Mol Biol. 2015; 52: 217–31. doi: 10.1165/rcmb.2013-0310OC PMID: 25029475

93. LeClair R, Lindner V. The role of collagen triple helix repeat containing 1 in injured arteries, collagen expression, and transforming growth factor beta signaling. Trends Cardiovasc Med. 2007; 17: 202–5. doi: 10.1016/j.tcm.2007.05.004 PMID: 17662915

94. Eriksson J, Le Joncour V, Nummela P, Jahkola T, Virolainen S, Laakkonen P, et al. Gene expression analyses of primary melanomas reveal CTHRC1 as an important player in melanoma progression. Oncotarget. 2016.

95. Wang CY, Zhang JJ, Hua L, Yao KH, Chen JT, Ren XQ. MicroRNA-98 suppresses cell proliferation, migration and invasion by targeting collagen triple helix repeat containing 1 in hepatocellular carcinoma. Mol Med Rep. 2016; 13: 2639–44. doi: 10.3892/mmr.2016.4833 PMID: 26846175

96. Ding Q, Zhang M, Liu C. Asporin participates in gastric cancer cell growth and migration by influencing EGF receptor signaling. Oncol Rep. 2015; 33: 1783–90. doi: 10.3892/or.2015.3791 PMID: 25673058

97. Hurley PJ, Sundi D, Shinder B, Simons BW, Hughes RM, Miller RM, et al. Germline Variants in Asporin Vary by Race, Modulate the Tumor Microenvironment, and Are Differentially Associated with Metastatic Prostate Cancer. Clin Cancer Res. 2016; 22: 448–58. doi: 10.1158/1078-0432.CCR-15-0256 PMID: 26446945

98. Shih B, McGrouther DA, Bayat A. Identification of novel keloid biomarkers through profiling of tissue biopsies versus cell cultures in keloid margin specimens compared to adjacent normal skin. Eplasty. 2010; 10: e24. PMID: 20418938

99. van Beuge MM, Ten Dam EJ, Werker PM, Bank RA. Wnt pathway in Dupuytren disease: connecting profibrotic signals. Transl Res. 2015; 166: 762–71 e3. doi: 10.1016/j.trsl.2015.09.006 PMID: 26470681

100. Jian YC, Wang JJ, Dong S, Hu JW, Hu LJ, Yang GM, et al. Wnt-induced secreted protein 1/CCN4 in liver fibrosis both in vitro and in vivo. Clin Lab. 2014; 60: 29–35. PMID: 24600972

101. Berschneider B, Ellwanger DC, Baarsma HA, Thiel C, Shimbori C, White ES, et al. miR-92a regulates TGF-beta1-induced WISP1 expression in pulmonary fibrosis. The international journal of biochemistry & cell biology. 2014; 53: 432–41.

102. Andrews JP, Marttala J, Macarak E, Rosenbloom J, Uitto J. Keloids: The paradigm of skin fibrosis—Pathomechanisms and treatment. Matrix Biol. 2016.

103. Wu CS, Wu PH, Fang AH, Lan CC. FK506 inhibits the enhancing effects of transforming growth factor (TGF)-beta1 on collagen expression and TGF-beta/Smad signalling in keloid fibroblasts: implication for new therapeutic approach. Br J Dermatol. 2012; 167: 532–41. doi: 10.1111/j.1365-2133.2012.11023.x PMID: 22540338

104. Katsuno Y, Lamouille S, Derynck R. TGF-beta signaling and epithelial-mesenchymal transition in cancer progression. Curr Opin Oncol. 2013; 25: 76–84. doi: 10.1097/CCO.0b013e32835b6371 PMID: 23197193

105. Derynck R, Muthusamy BP, Saeteurn KY. Signaling pathway cooperation in TGF-beta-induced epithelial-mesenchymal transition. Curr Opin Cell Biol. 2014; 31: 56–66. doi: 10.1016/j.ceb.2014.09.001 PMID: 25240174

106. Strzyz P. Cancer biology: TGF [beta] and EMT as double agents. Nature Reviews Molecular Cell Biology. 2016.

107. David CJ, Huang Y-H, Chen M, Su J, Zou Y, Bardeesy N, et al. TGF-β Tumor Suppression through a Lethal EMT. Cell. 2016; 164: 1015–30. doi: 10.1016/j.cell.2016.01.009 PMID: 26898331

108. Valcourt U, Carthy J, Okita Y, Alcaraz L, Kato M, Thuault S, et al. Analysis of Epithelial–Mesenchymal Transition Induced by Transforming Growth Factor β. TGF-β Signaling: Methods and Protocols. 2016: 147–81.

109. Eming SA, Krieg T, Davidson JM. Inflammation in wound repair: molecular and cellular mechanisms. The Journal of investigative dermatology. 2007; 127: 514–25. doi: 10.1038/sj.jid.5700701 PMID: 17299434

110. Qian LW, Fourcaudot AB, Yamane K, You T, Chan RK, Leung KP. Exacerbated and prolonged inflammation impairs wound healing and increases scarring. Wound repair and regeneration: official publication of the Wound Healing Society [and] the European Tissue Repair Society. 2016; 24: 26–34.

111. Zhang M, Xu Y, Liu Y, Cheng Y, Zhao P, Liu H, et al. Chemokine-Like Factor 1 (CKLF-1) is Overexpressed in Keloid Patients: A Potential Indicating Factor for Keloid-Predisposed Individuals. Medicine (Baltimore). 2016; 95: e3082.

112. Dong X, Mao S, Wen H. Upregulation of proinflammatory genes in skin lesions may be the cause of keloid formation (Review). Biomed Rep. 2013; 1: 833–6. doi: 10.3892/br.2013.169 PMID: 24649037

113. Borthwick LA, Wynn TA. IL-13 and TGF-β1: Core Mediators of Fibrosis. Current Pathobiology Reports. 2015; 3: 273–82.

114. Baraut J, Farge D, Jean-Louis F, Masse I, Grigore EI, Arruda LC, et al. Transforming growth factor-beta increases interleukin-13 synthesis via GATA-3 transcription factor in T-lymphocytes from patients with systemic sclerosis. Arthritis Res Ther. 2015; 17: 196. doi: 10.1186/s13075-015-0708-0 PMID: 26227022

115. Oriente A, Fedarko NS, Pacocha SE, Huang SK, Lichtenstein LM, Essayan DM. Interleukin-13 modulates collagen homeostasis in human skin and keloid fibroblasts. J Pharmacol Exp Ther. 2000; 292: 988–94. PMID: 10688614

116. McCormick SM, Heller NM. Commentary: IL-4 and IL-13 receptors and signaling. Cytokine. 2015; 75: 38–50. doi: 10.1016/j.cyto.2015.05.023 PMID: 26187331

117. Granel B, Allanore Y, Chevillard C, Arnaud V, Marquet S, Weiller PJ, et al. IL13RA2 gene polymorphisms are associated with systemic sclerosis. J Rheumatol. 2006; 33: 2015–9. PMID: 16981293

118. Chiaramonte MG, Mentink-Kane M, Jacobson BA, Cheever AW, Whitters MJ, Goad ME, et al. Regulation and function of the interleukin 13 receptor alpha 2 during a T helper cell type 2-dominant immune response. J Exp Med. 2003; 197: 687–701. doi: 10.1084/jem.20020903 PMID: 12642601

119. Wood N, Whitters MJ, Jacobson BA, Witek J, Sypek JP, Kasaian M, et al. Enhanced interleukin (IL)-13 responses in mice lacking IL-13 receptor alpha 2. J Exp Med. 2003; 197: 703–9. doi: 10.1084/jem.20020906 PMID: 12642602

120. Keane MP, Gomperts BN, Weigt S, Xue YY, Burdick MD, Nakamura H, et al. IL-13 is pivotal in the fibro-obliterative process of bronchiolitis obliterans syndrome. J Immunol. 2007; 178: 511–9. PMID: 17182591

121. Kolodsick JE, Toews GB, Jakubzick C, Hogaboam C, Moore TA, McKenzie A, et al. Protection from fluorescein isothiocyanate-induced fibrosis in IL-13-deficient, but not IL-4-deficient, mice results from impaired collagen synthesis by fibroblasts. J Immunol. 2004; 172: 4068–76. PMID: 15034018

122. Charrad R, Berraies A, Hamdi B, Ammar J, Hamzaoui K, Hamzaoui A. Anti-inflammatory activity of IL-37 in asthmatic children: Correlation with inflammatory cytokines TNF-alpha, IL-beta, IL-6 and IL-17A. Immunobiology. 2016; 221: 182–7. doi: 10.1016/j.imbio.2015.09.009 PMID: 26454413

123. Imaeda H, Takahashi K, Fujimoto T, Kasumi E, Ban H, Bamba S, et al. Epithelial expression of interleukin-37b in inflammatory bowel disease. Clin Exp Immunol. 2013; 172: 410–6. doi: 10.1111/cei.12061 PMID: 23600829

124. Chen Z, O'Shea JJ. Regulation of IL-17 production in human lymphocytes. Cytokine. 2008; 41: 71–8. doi: 10.1016/j.cyto.2007.09.009 PMID: 17981475

125. Benevides L, da Fonseca DM, Donate PB, Tiezzi DG, De Carvalho DD, de Andrade JM, et al. IL17 Promotes Mammary Tumor Progression by Changing the Behavior of Tumor Cells and Eliciting Tumorigenic Neutrophils Recruitment. Cancer Res. 2015; 75: 3788–99. doi: 10.1158/0008-5472.CAN-15-0054 PMID: 26208902

126. Isailovic N, Daigo K, Mantovani A, Selmi C. Interleukin-17 and innate immunity in infections and chronic inflammation. J Autoimmun. 2015; 60: 1–11. doi: 10.1016/j.jaut.2015.04.006 PMID: 25998834

127. Loubaki L, Hadj-Salem I, Fakhfakh R, Jacques E, Plante S, Boisvert M, et al. Co-culture of human bronchial fibroblasts and CD4+ T cells increases Th17 cytokine signature. PloS one. 2013; 8: e81983. doi: 10.1371/journal.pone.0081983 PMID: 24349168

128. Qu M, Song N, Chai G, Wu X, Liu W. Pathological niche environment transforms dermal stem cells to keloid stem cells: a hypothesis of keloid formation and development. Med Hypotheses. 2013; 81: 807–12. doi: 10.1016/j.mehy.2013.08.033 PMID: 24074897

129. Gu FM, Li QL, Gao Q, Jiang JH, Zhu K, Huang XY, et al. IL-17 induces AKT-dependent IL-6/JAK2/STAT3 activation and tumor progression in hepatocellular carcinoma. Mol Cancer. 2011; 10: 150. doi: 10.1186/1476-4598-10-150 PMID: 22171994

130. Jadidi-Niaragh F, Ghalamfarsa G, Memarian A, Asgarian-Omran H, Razavi SM, Sarrafnejad A, et al. Downregulation of IL-17-producing T cells is associated with regulatory T cell expansion and disease progression in chronic lymphocytic leukemia. Tumour Biol. 2013; 34: 929–40. doi: 10.1007/s13277-012-0628-4 PMID: 23269607

131. Francois A, Gombault A, Villeret B, Alsaleh G, Fanny M, Gasse P, et al. B cell activating factor is central to bleomycin- and IL-17-mediated experimental pulmonary fibrosis. J Autoimmun. 2015; 56: 1–11. doi: 10.1016/j.jaut.2014.08.003 PMID: 25441030

132. Wang L, Chen S, Xu K. IL-17 expression is correlated with hepatitis Brelated liver diseases and fibrosis. Int J Mol Med. 2011; 27: 385–92. doi: 10.3892/ijmm.2011.594 PMID: 21225222

133. Okamoto Y, Hasegawa M, Matsushita T, Hamaguchi Y, Huu DL, Iwakura Y, et al. Potential roles of interleukin-17A in the development of skin fibrosis in mice. Arthritis & Rheumatism. 2012; 64: 3726–35.

134. Nittka S, Gunther J, Ebisch C, Erbersdobler A, Neumaier M. The human tumor suppressor CEACAM1 modulates apoptosis and is implicated in early colorectal tumorigenesis. Oncogene. 2004; 23: 9306–13. doi: 10.1038/sj.onc.1208259 PMID: 15568039

135. Cruz PV, Wakai T, Shirai Y, Yokoyama N, Hatakeyama K. Loss of carcinoembryonic antigen-related cell adhesion molecule 1 expression is an adverse prognostic factor in hepatocellular carcinoma. Cancer. 2005; 104: 354–60. doi: 10.1002/cncr.21159 PMID: 15952183

136. Busch C, Hanssen TA, Wagener C, B OB. Down-regulation of CEACAM1 in human prostate cancer: correlation with loss of cell polarity, increased proliferation rate, and Gleason grade 3 to 4 transition. Hum Pathol. 2002; 33: 290–8. PMID: 11979369

137. Oliveira-Ferrer L, Tilki D, Ziegeler G, Hauschild J, Loges S, Irmak S, et al. Dual role of carcinoembryonic antigen-related cell adhesion molecule 1 in angiogenesis and invasion of human urinary bladder cancer. Cancer Res. 2004; 64: 8932–8. doi: 10.1158/0008-5472.CAN-04-0505 PMID: 15604255

138. Ashkenazi S, Ortenberg R, Besser M, Schachter J, Markel G. SOX9 indirectly regulates CEACAM1 expression and immune resistance in melanoma cells. Oncotarget. 2016.

139. Zalzali H, Naudin C, Bastide P, Quittau-Prevostel C, Yaghi C, Poulat F, et al. CEACAM1, a SOX9 direct transcriptional target identified in the colon epithelium. Oncogene. 2008; 27: 7131–8. doi: 10.1038/onc.2008.331 PMID: 18794798

140. Roda G, Dahan S, Mezzanotte L, Caponi A, Roth-Walter F, Pinn D, et al. Defect in CEACAM family member expression in Crohn's disease IECs is regulated by the transcription factor SOX9. Inflamm Bowel Dis. 2009; 15: 1775–83. doi: 10.1002/ibd.21023 PMID: 19637360

141. Yan C, Boyd DD. ATF3 regulates the stability of p53: a link to cancer. Cell Cycle. 2006; 5: 926–9. doi: 10.4161/cc.5.9.2714 PMID: 16628010

142. Hackl C, Lang SA, Moser C, Mori A, Fichtner-Feigl S, Hellerbrand C, et al. Activating transcription factor-3 (ATF3) functions as a tumor suppressor in colon cancer and is up-regulated upon heat-shock protein 90 (Hsp90) inhibition. BMC Cancer. 2010; 10: 668. doi: 10.1186/1471-2407-10-668 PMID: 21129190

143. Zhou H, Yuan Y, Ni J, Guo H, Deng W, Bian ZY, et al. Pleiotropic and puzzling effects of ATF3 in maladaptive cardiac remodeling. Int J Cardiol. 2016; 206: 87–8. doi: 10.1016/j.ijcard.2016.01.143 PMID: 26780683

144. Huang X, Li X, Guo B. KLF6 induces apoptosis in prostate cancer cells through up-regulation of ATF3. The Journal of biological chemistry. 2008; 283: 29795–801. doi: 10.1074/jbc.M802515200 PMID: 18755691

145. Xie JJ, Xie YM, Chen B, Pan F, Guo JC, Zhao Q, et al. ATF3 functions as a novel tumor suppressor with prognostic significance in esophageal squamous cell carcinoma. Oncotarget. 2014; 5: 8569–82. doi: 10.18632/oncotarget.2322 PMID: 25149542

146. Eo HJ, Kwon TH, Park GH, Song HM, Lee SJ, Park NH, et al. In Vitro Anticancer Activity of Phlorofucofuroeckol A via Upregulation of Activating Transcription Factor 3 against Human Colorectal Cancer Cells. Mar Drugs. 2016;14.

147. Jiliang S, Hui L, Gonghui L, Renan J, Liang S, Mingming C, et al. TR4 nuclear receptor enhances the cisplatin chemo-sensitivity via altering the ATF3 expression to better suppress HCC cell growth. Oncotarget. 2016.

148. Song HM, Park GH, Eo HJ, Jeong JB. Naringenin-Mediated ATF3 Expression Contributes to Apoptosis in Human Colon Cancer. Biomol Ther (Seoul). 2016; 24: 140–6.

149. Meech R, Rogers A, Zhuang L, Lewis BC, Miners JO, Mackenzie PI. Identification of residues that confer sugar selectivity to UDP-glycosyltransferase 3A (UGT3A) enzymes. The Journal of biological chemistry. 2012; 287: 24122–30. doi: 10.1074/jbc.M112.343608 PMID: 22621930

150. MacKenzie PI, Rogers A, Elliot DJ, Chau N, Hulin JA, Miners JO, et al. The novel UDP glycosyltransferase 3A2: cloning, catalytic properties, and tissue distribution. Mol Pharmacol. 2011; 79: 472–8. doi: 10.1124/mol.110.069336 PMID: 21088224

151. Morikawa Y, Kezuka C, Endo S, Ikari A, Soda M, Yamamura K, et al. Acquisition of doxorubicin resistance facilitates migrating and invasive potentials of gastric cancer MKN45 cells through up-regulating

aldo-keto reductase 1B10. Chem Biol Interact. 2015; 230: 30–9. doi: 10.1016/j.cbi.2015.02.005 PMID: 25686905

152. Januchowski R, Wojtowicz K, Zabel M. The role of aldehyde dehydrogenase (ALDH) in cancer drug resistance. Biomed Pharmacother. 2013; 67: 669–80. doi: 10.1016/j.biopha.2013.04.005 PMID: 23721823

153. Nwabo Kamdje AH, Bassi G, Pacelli L, Malpeli G, Amati E, Nichele I, et al. Role of stromal cell-mediated Notch signaling in CLL resistance to chemotherapy. Blood Cancer J. 2012; 2: e73. doi: 10.1038/bcj.2012.17 PMID: 22829975

154. Simoes BM, O'Brien CS, Eyre R, Silva A, Yu L, Sarmiento-Castro A, et al. Anti-estrogen Resistance in Human Breast Tumors Is Driven by JAG1-NOTCH4-Dependent Cancer Stem Cell Activity. Cell Rep. 2015; 12: 1968–77. doi: 10.1016/j.celrep.2015.08.050 PMID: 26387946

155. Honoki K, Fujii H, Kubo A, Kido A, Mori T, Tanaka Y, et al. Possible involvement of stem-like populations with elevated ALDH1 in sarcomas for chemotherapeutic drug resistance. Oncol Rep. 2010; 24: 501–5. PMID: 20596639

156. Whitman M, Hunter DG, Engle EC. Congenital Fibrosis of the Extraocular Muscles. In: Pagon RA, Adam MP, Ardinger HH, Wallace SE, Amemiya A, Bean LJH, et al., editors. GeneReviews(R). Seattle (WA)1993.

157. Leandro-Garcia LJ, Leskela S, Landa I, Montero-Conde C, Lopez-Jimenez E, Leton R, et al. Tumoral and tissue-specific expression of the major human beta-tubulin isotypes. Cytoskeleton (Hoboken). 2010; 67: 214–23.

158. Lebok P, Ozturk M, Heilenkotter U, Jaenicke F, Muller V, Paluchowski P, et al. High levels of class III beta-tubulin expression are associated with aggressive tumor features in breast cancer. Oncol Lett. 2016; 11: 1987–94. doi: 10.3892/ol.2016.4206 PMID: 26998111

159. Miyamoto A, Akasaka K, Oikawa H, Akasaka T, Masuda T, Maesawa C. Immunohistochemical study of HER2 and TUBB3 proteins in extramammary Paget disease. Am J Dermatopathol. 2010; 32: 578–85. doi: 10.1097/DAD.0b013e3181cd35e0 PMID: 20534991

160. McCarroll JA, Gan PP, Erlich RB, Liu M, Dwarte T, Sagnella SS, et al. TUBB3/betaIII-tubulin acts through the PTEN/AKT signaling axis to promote tumorigenesis and anoikis resistance in non-small cell lung cancer. Cancer Res. 2015; 75: 415–25. doi: 10.1158/0008-5472.CAN-14-2740 PMID: 25414139

161. Tsourlakis MC, Weigand P, Grupp K, Kluth M, Steurer S, Schlomm T, et al. betaIII-tubulin overexpression is an independent predictor of prostate cancer progression tightly linked to ERG fusion status and PTEN deletion. Am J Pathol. 2014; 184: 609–17. doi: 10.1016/j.ajpath.2013.11.007 PMID: 24378408

162. Raspaglio G, Petrillo M, Martinelli E, Puma DDL, Mariani M, De Donato M, et al. Sox9 and Hif-2α regulate TUBB3 gene expression and affect ovarian cancer aggressiveness. Gene. 2014; 542: 173–81. doi: 10.1016/j.gene.2014.03.037 PMID: 24661907

163. Duran GE, Wang YC, Francisco EB, Rose JC, Martinez FJ, Coller J, et al. Mechanisms of resistance to cabazitaxel. Mol Cancer Ther. 2015; 14: 193–201. doi: 10.1158/1535-7163.MCT-14-0155 PMID: 25416788

164. Ferrandina G, Zannoni GF, Martinelli E, Paglia A, Gallotta V, Mozzetti S, et al. Class III beta-tubulin overexpression is a marker of poor clinical outcome in advanced ovarian cancer patients. Clin Cancer Res. 2006; 12: 2774–9. doi: 10.1158/1078-0432.CCR-05-2715 PMID: 16675570

165. Mariani M, Shahabi S, Sieber S, Scambia G, Ferlini C. Class III β-tubulin (TUBB3): more than a biomarker in solid tumors? Current molecular medicine. 2011; 11: 726–31. PMID: 21999149

166. Zhang Z, Nie F, Kang C, Chen B, Qin Z, Ma J, et al. Increased periostin expression affects the proliferation, collagen synthesis, migration and invasion of keloid fibroblasts under hypoxic conditions. Int J Mol Med. 2014; 34: 253–61. doi: 10.3892/ijmm.2014.1760 PMID: 24788198

167. Touchi R, Ueda K, Kurokawa N, Tsuji M. Central regions of keloids are severely ischaemic. Journal of plastic, reconstructive & aesthetic surgery: JPRAS. 2016; 69: e35–41.

168. Jones CD, Guiot L, Samy M, Gorman M, Tehrani H. The Use of Chemotherapeutics for the Treatment of Keloid Scars. Dermatol Reports. 2015; 7: 5880. doi: 10.4081/dr.2015.5880 PMID: 26236447

169. van Leeuwen MC, Stokmans SC, Bulstra AE, Meijer OW, Heymans MW, Ket JC, et al. Surgical Excision with Adjuvant Irradiation for Treatment of Keloid Scars: A Systematic Review. Plast Reconstr Surg Glob Open. 2015; 3: e440. doi: 10.1097/GOX.0000000000000357 PMID: 26301129

170. Arno AI, Gauglitz GG, Barret JP, Jeschke MG. Up-to-date approach to manage keloids and hypertrophic scars: a useful guide. Burns. 2014; 40: 1255–66. doi: 10.1016/j.burns.2014.02.011 PMID: 24767715

171. Song N, Wu X, Gao Z, Zhou G, Zhang WJ, Liu W. Enhanced expression of membrane transporter and drug resistance in keloid fibroblasts. Hum Pathol. 2012; 43: 2024–32. doi: 10.1016/j.humpath.2011.12.026 PMID: 22617232

172. Moon J-H, Kwak SS, Park G, Jung H-Y, Yoon BS, Park J, et al. Isolation and characterization of multipotent human keloid-derived mesenchymal-like stem cells. Stem cells and development. 2008; 17: 713–24. doi: 10.1089/scd.2007.0210 PMID: 18710345

173. Clavel G, Thiolat A, Boissier MC. Interleukin newcomers creating new numbers in rheumatology: IL-34 to IL-38. Joint Bone Spine. 2013; 80: 449–53. doi: 10.1016/j.jbspin.2013.04.014 PMID: 23849463

174. Singh A, Settleman J. EMT, cancer stem cells and drug resistance: an emerging axis of evil in the war on cancer. Oncogene. 2010; 29: 4741–51. doi: 10.1038/onc.2010.215 PMID: 20531305

175. El-Serag H.B., et al., *Gene expression in Barrett's esophagus*: *laser capture versus whole tissue*. Scand J Gastroenterol, 2009. 44(7): p. 787–95. doi: 10.1080/00365520902898127 PMID: 19391063

176. De Marchi T., et al., The advantage of laser-capture microdissection over whole tissue analysis in proteomic profiling studies. Proteomics, 2016. 16(10): p. 1474–85. doi: 10.1002/pmic.201600004 PMID: 27030549

177. Zheng J., et al., Laser capture microdissected mucosa versus whole tissue specimens for assessment of radiation-induced dynamic molecular and pathway changes in the small intestine. PLoS One, 2013. 8(1): p. e53711. doi: 10.1371/journal.pone.0053711 PMID: 23341980

178. Shekouh A.R., et al., Application of laser capture microdissection combined with two-dimensional electrophoresis for the discovery of differentially regulated proteins in pancreatic ductal adenocarcinoma. Proteomics, 2003. 3(10): p. 1988–2001. doi: 10.1002/pmic.200300466 PMID: 14625861